2010

Reducing phase noise degradation due to vibration of crystal oscillators

Cory Nelson
Iowa State University

Reducing phase noise degradation due to vibration of crystal oscillators

by

Cory Lee Nelson

A thesis submitted to the graduate faculty

in partial fulfillment of the requirements for the degree of

MASTER OF SCIENCE

Major: Electrical Engineering

Program of Study Committee:
Mani Mina, Major Professor
Robert Weber
Jaeyoun Kim

Iowa State University

Ames, Iowa

2010

Table of Contents

List of Figures

List of Tables

Acknowledgements

Throughout the entire research process, I have received dedicated support from professors and colleagues at Rockwell Collins Inc. The guidance I have received from my major professor Mani Mina along with Robert Weber has been exceptional. Without their help I wouldn't have been able to turn my research into a thesis.

I would also like to thank the tireless efforts of both Mark Yu and Henry Eniola, whose knowledge and aide helped me along with the research and testing that I was able to do at Rockwell Collins.

In addition I would like to thank my parents Robert and Mary Nelson. Their encouragement towards my education from an early age has kept me striving for knowledge even when settled into a career. And my sister Beth who always encouraged me to dress for success even when it seems success will never come.

Abstract

In the radio communications industry, one major problem is the vibration induced on to a frequency standard. The most commonly used frequency standard is the crystal oscillator; as the crystal oscillator gets vibrated with varying force and frequencies of vibration the phase noise of the signal changes. As the phase noise increases, the signal to noise ratio decreases causing the likelihood of transmitting or receiving an incorrect signal to rise. This makes it critical to limit the phase noise increase that occurs in the frequency standard of the system.

Mechanical isolation systems have been implemented in the industry to limit the system vibration that propagates to the frequency standard. These systems add weight and size to the overall design, which make them not ideal for all applications. For systems that can not use isolators, open loop cancellation has been implemented in past designs. This cancellation measures the vibration and subtracts it from the phase noise, but such a system has drawbacks with changes in vibration frequency and force. A closed loop design is suggested to correct this.

In order to maximize performance an IQ modulation feedback system was designed. The feedback system utilizes information about both the vibration and the measured phase noise. It uses these two inputs concurrently to correct the output frequency of the crystal as it changes with vibration. In order to reduce the space and weight of the design, mechanical vibration dampeners were removed.

After various tests and simulations it was determined that using this feedback to the oscillator could correct the oscillator's frequency change based on the vibration experienced. This would reduce the phase noise of the oscillator compared to an oscillator vibrated without any compensation. Using this compensation system would reduce the overall phase noise of any communication system currently in use that utilizes crystal oscillators.

1 Introduction

As a crystal oscillator undergoes vibration in a communication system the signal degrades from the added phase noise. In order to transmit and receive data correctly, this phase noise needs to be lowered or the probability of an incorrect data sequence being received will increase. This increases the need to limit the amount of vibration on the crystal oscillator.

The technology behind the field of radio communications is rapidly growing. As required throughput increase and the locations of radios become more exotic, the signal needs to become clearer in order to assure the accuracy of data being received. A prime source of the system's signal quality and creation is the local oscillator.

1.1 Crystal Oscillators

Crystal oscillators use a vibrating piezoelectric material's mechanical resonance to create a voltage at a precise frequency. The name crystal oscillator comes from the most commonly used piezoelectric substance, a quartz crystal. The generated voltage can be used for many applications, including a reference frequency for communication systems.

Quartz crystals have a very high level of physical and chemical stability to go along with a very small elastic hysteresis. This allows the crystals to be used in numerous applications while requiring minimal energy input to sustain oscillation.

The piezoelectric effect was discovered in 1880 by Jacques and Pierre Curie. The piezoelectric effect shows that if a crystal is stressed it will create an electric potential between a pair of conductors surrounding the crystal. Inversely, if a crystal is placed within an electric field it will be deformed an amount which is relative to the strength of the field. This affect was first applied to a quartz resonator in 1925 by K.S. Van Dyke [1]. K.S. Van Dyke's design consisted of a quartz resonator mounted between two

conducting electrodes. The electrical connection is applied to these conducting electrodes. When connected to any circuit, a crystal resonator and an electrical circuit equivalent resonator will be electrically identical at frequencies close to the crystal resonator's resonant frequency.

The Van Dyke principal was applied to controlling a frequency in a vacuum tube circuit in 1922 by Walter G. Cady. Using the oscillator shown in Figure 1-1, Cady was able to add an equivalent RLC circuit to create the first ever crystal oscillator.

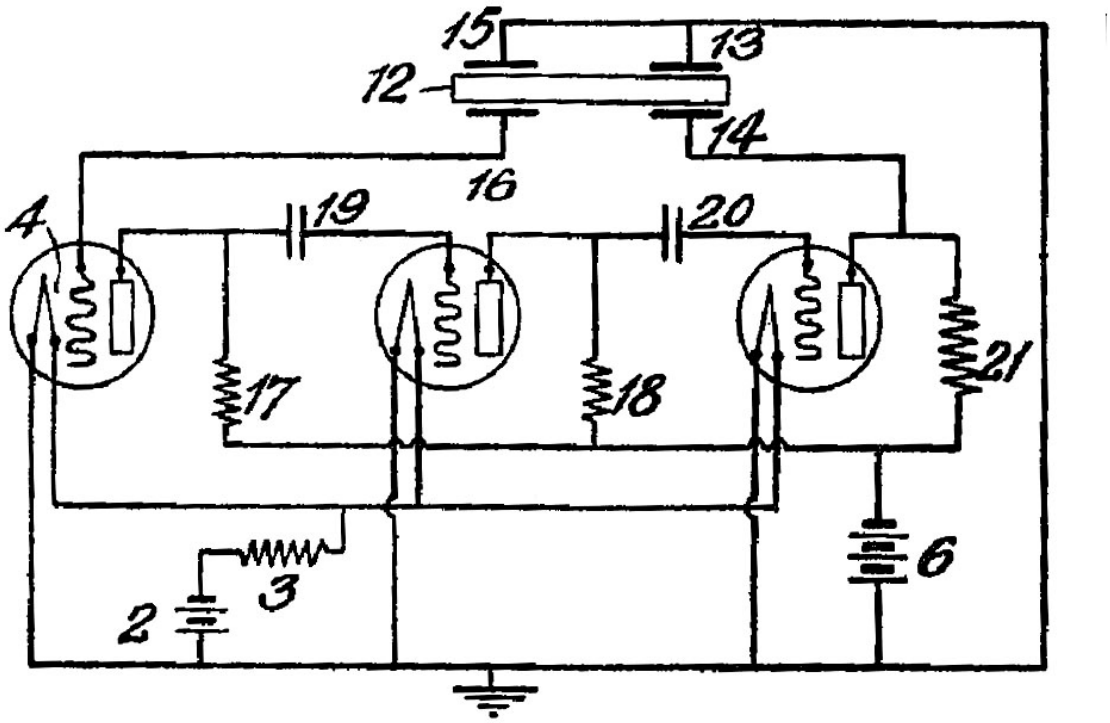

Figure 1-1 Walter G. Cady's Design for a Crystal Oscillator in 1922 [3]

This work was later expanded by George Washington Pierce [4] who simplified the Cady design to only one vacuum tube and a one-port crystal resonator, Figure 1-2. Pierce also showed that plates of the quartz, if cut differently, could control the frequency's properties. Working together, they were able to show that while standard LC oscillators maintain a frequency within a 1% tolerance band, the quartz controlled oscillators could maintain a frequency tolerance of a hundred times better than that. [2]

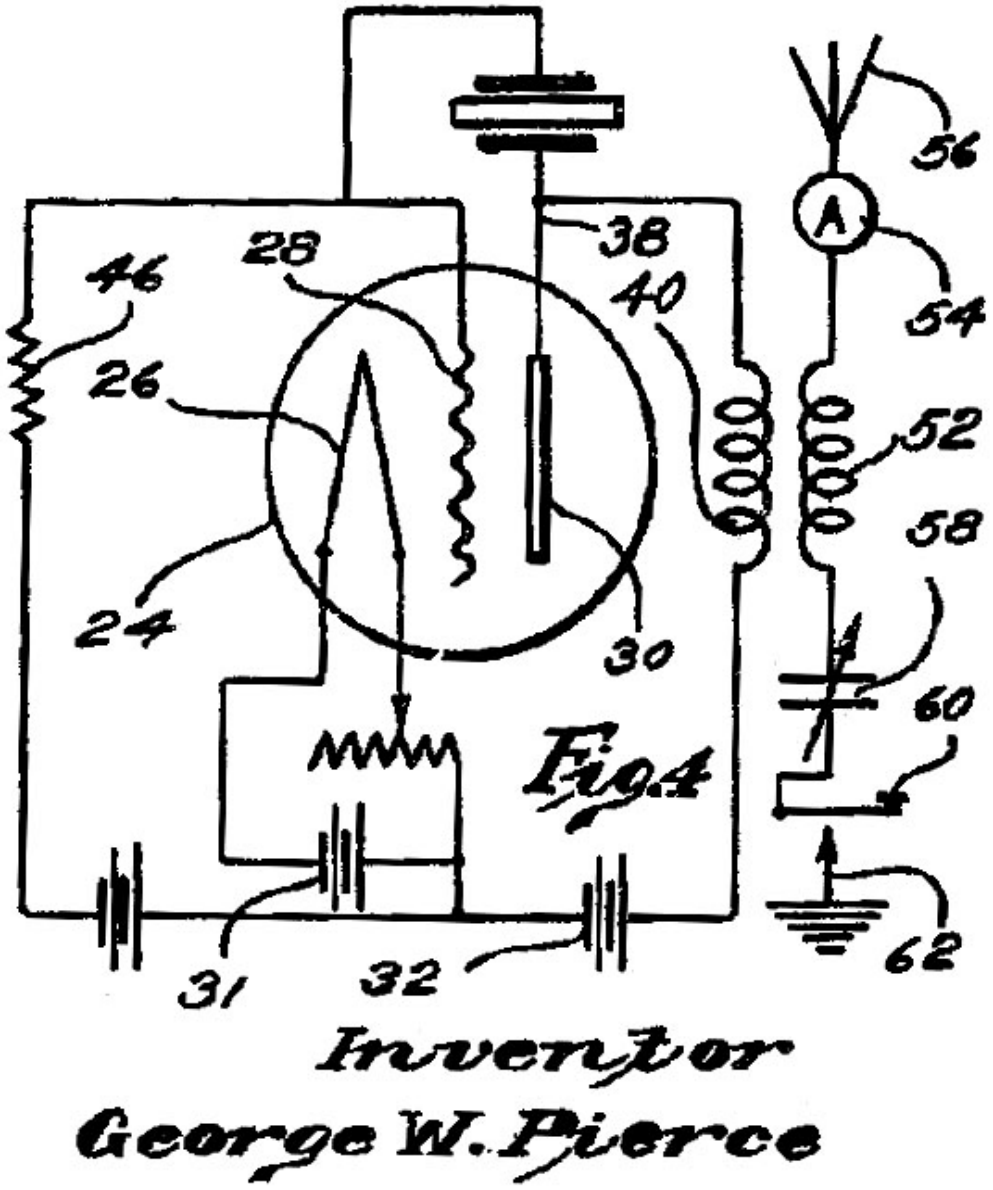

Figure 1-2 Pierce's Crystal Oscillator design with one-port crystal resonator [4]

Using these advancements, crystal oscillators quickly became a standard for use in most applications. The frequency stability became of greater importance in designs for communication systems. With this greater frequency stability came a greater impact of the phase noise of the system.

1.2 Phase Noise

Phase noise is defined as the rapid, short-term, random fluctuations in the phase of the wave in the frequency domain; this can be caused by time domain instabilities known as jitter. Generally speaking, an ideal noise-free signal would be represented as:

$$v(t) = A * \cos(2\pi f_o t) \quad \text{[Equation II-1]}$$

Where A is the amplitude of the signal in the time domain and f_o is the frequency of oscillation. Phase noise could be added to this system by adding in a stochastic process. This is represented by φ in the following signal:

$$v(t) = A * \cos(2\pi f_o t + \varphi(t)) \quad \text{[Equation II-2]}$$

In the frequency domain, the ideal signal would be a single line at f_o. The phase noise adds power in the sidebands. A representation of this is shown in Figure 1-3 below.

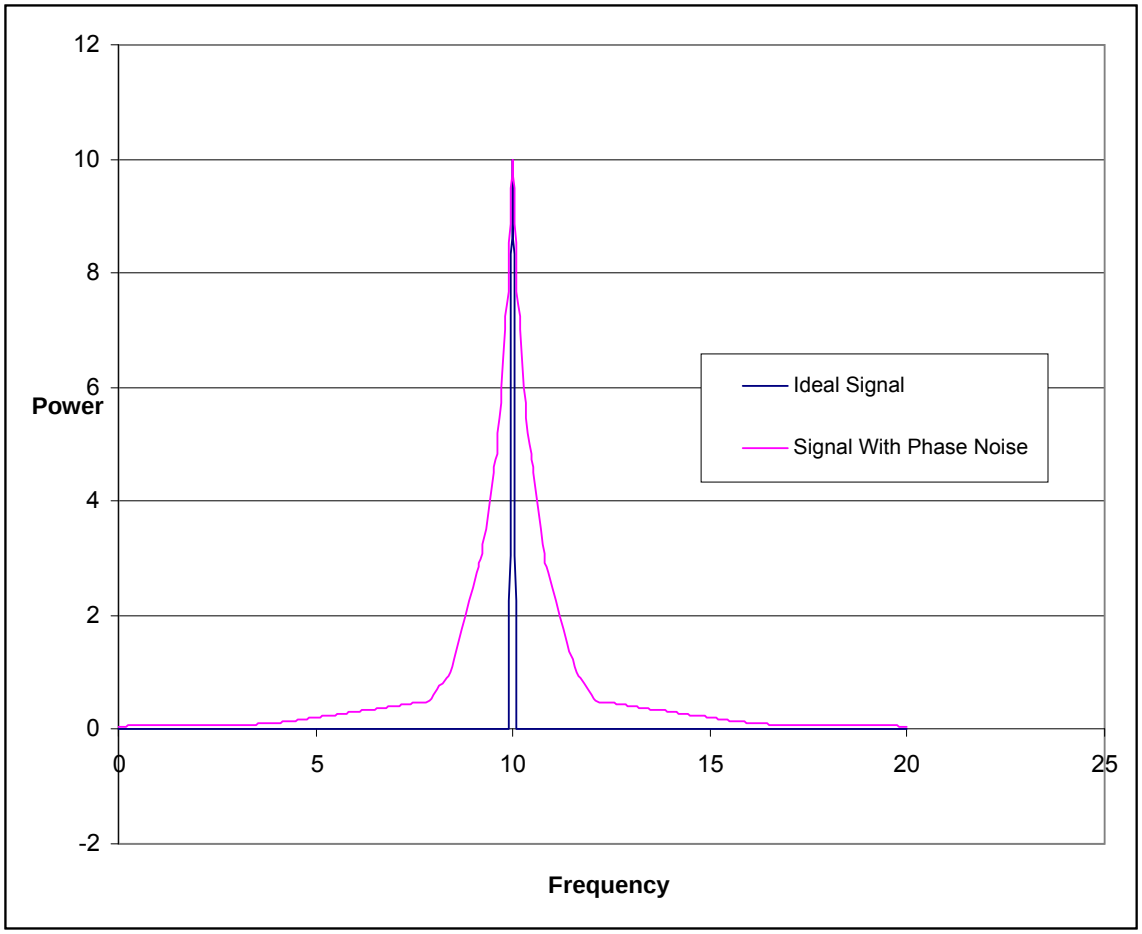

Figure 1-3 Frequency Domain Signal and Phase Noise Depiction

The way to calculate the single side band phase noise of the oscillator in terms of dBc/Hz, which is what most measurement tools will use, is as follows:

$$SSB(\Delta f) = 10 * \log(\frac{P_S(f_0)}{P_{SSB}(f_0 \pm \Delta f)}) \quad \text{[Equation II-3]}$$

In this equation, P_S is the power of the signal at f_o and P_{SSB} is the power in the single sideband at a frequency Δf from f_o. The term dBc/Hz refers to power in a 1 Hz bandwidth being so many dB below the carrier power at f_o. This equation gives the Single Side Band Phase Noise with respect to the carrier power. [5]

1.3 Vibration

Under acceleration, quartz crystal oscillators change frequency slightly. Any movement or change in forces on the crystal can change the frequency. This is typically represented by the vendor as the Hz per g number. In general, a 10 MHz crystal will change about 0.01 Hz per g.

The sensitivity means that crystals installed in equipment exposed to mechanical vibration will have a higher phase noise due to these random slight changes in frequency. This occurs in helicopters, jets, or even in location in close proximity to other mechanical vibrating elements like a cooling fan.

The effect of the sensitivity of the crystal with respect to the frequency of vibration can be calculated by the following equation. In this equation, "s" is the acceleration sensitivity of the crystal, "a" is the acceleration seen by the crystal, "f_o" is the frequency of oscillation and "f_v" is the frequency of mechanical vibration. The acceleration vector is the g level for a sine wave vibration, or the square root of twice the power spectral density in a one hertz bandwidth for random vibration. [6]

$$L(f) = 20 * \log(\frac{s * a * f_o}{2 * f_v}), dB \qquad \text{[Equation II-4]}$$

This means that a system with the 10 MHz crystal with 0.01 Hz/g sensitivity that experiences a 0.01 g^2/Hz level of acceleration will see approximately 40 dB degradation of the phase noise. To help correct for this problem it is important to understand what type of accelerations are occurring on the system.

1.4 Accelerometer

Accelerometers are electromechanical devices that measure the acceleration forces exerted upon them. There are two main types of acceleration that these measure, static and dynamic.

Static force is the force that is experienced due to gravity relative to earth's surface. In a circuit this force is described as the tilt experienced. As the circuitry moves relative to the earth's surface, the force upon it will be acting in a different way. This force can affect the crystal oscillator's performance because this will modulate the crystal frequency depending on the direction of the resultant force and the direction of the g sensitivity of the crystal. This typically means that the output of the crystal will change by a certain offset in Hz based on the Hz per g sensitivity of the crystal.

Dynamic forces are the forces experienced due to the acceleration of the circuit. This includes the vibration felt by the crystal oscillator. How vibration affects the oscillator and creates increased phase noise was discussed in the previous section.

Accelerometers can be built in a few different ways. The general idea behind an accelerometer is that it will produce a change in a circuit variable at a static position and output a voltage based on that. Two common ways to do this are with a piezoelectric crystal or with a capacitance.

The piezoelectric crystal uses the same theory as the crystal oscillator. When a crystal is put into the system that experiences forces on it based on the vibration or tilt of the crystal with respect to an acceleration vector the crystal will be stressed. As forces stress the crystal in the system, a voltage will be generated to match the level of stress upon the crystal. This voltage is then an indication of the amount of force on the crystal at any time. An example of a piezoelectric crystal is shown in Figure 1-4.

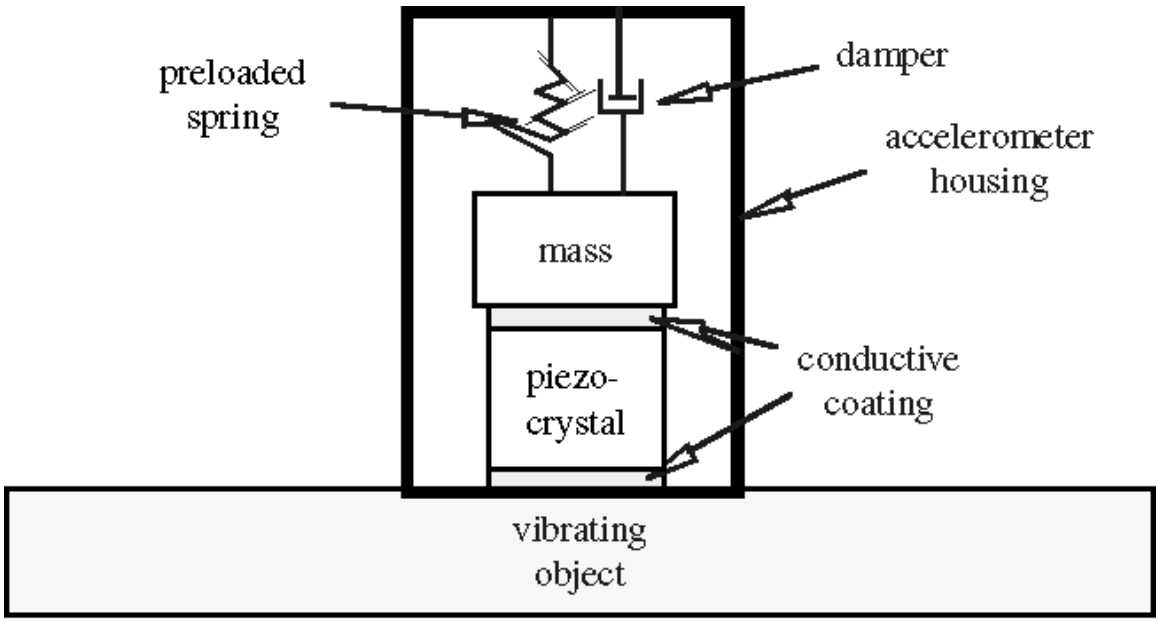

Figure 1-4 Piezoelectric Crystal Accelerometer [8]

A capacitance accelerometer uses a similar setup. For this circuit a capacitor with two plates is set up. As the forces on the system change, the plates shift relative to the strength of the force. This change alters the relative capacitance as the distance between the plates varies, causing a voltage change in the system, which can be used to measure the relative amount of force on the system. This can be seen in Figure 1-5. [9]

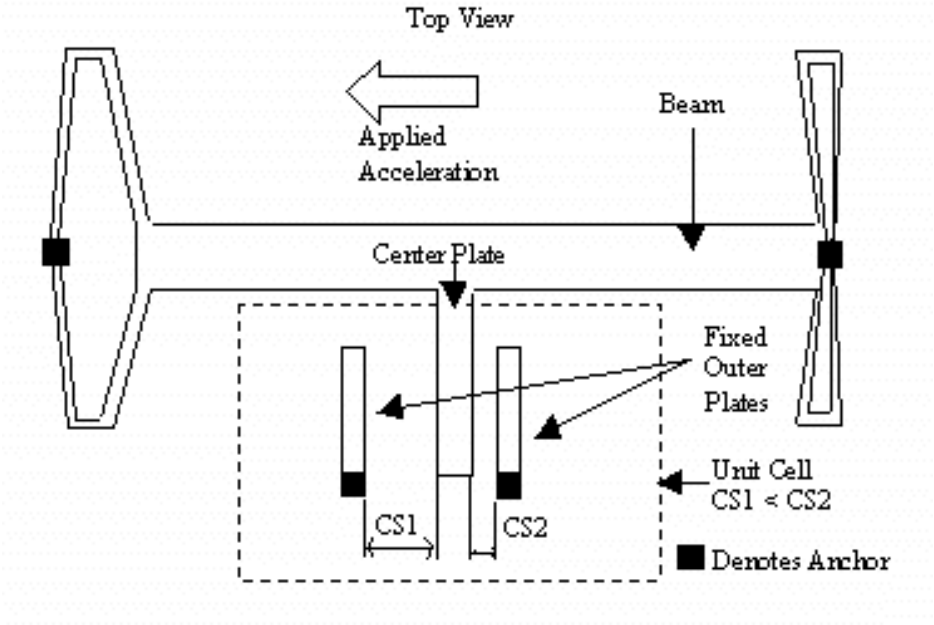

Figure 1-5 Capacitance Based Accelerometer [9]

1.5 IQ Modulation

IQ modulation is a technique that involves using two components of a vector signal: the "I" component and the "Q" component. The "I" stands for in-phase, while the "Q" stands for the quadrature component. This means when a signal changes frequency it can be represented by both a real and imaginary change. This real and imaginary change corresponds to the "I" and the "Q" signals of the system. A receiver can then be built that locks to the carrier frequency to read the data from the "I" and the "Q" signals as shown in Figure 1-6.

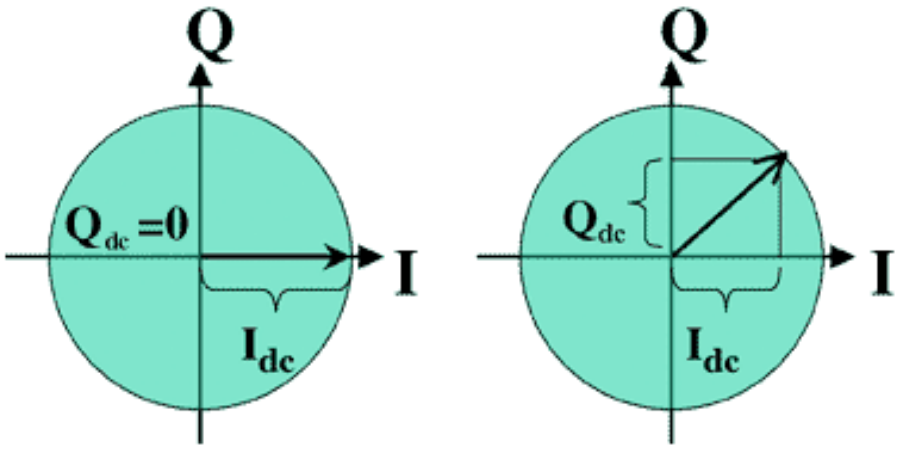

Figure 1-6 Polar Plot of IQ modulation example [10]

I and Q modulation is used most commonly with two orthogonal data streams modulated onto a common carrier. If the phases and the amplitudes are the same with the carrier then one of the sidebands would be cancelled out. If no DC Bias feeds through, then the carrier is also cancelled. The equations below are shown with DC Bias added to the "I" channel. This effect is usually removed with a low pass filter assuring that the carrier will be cancelled out. In the following (I) is In-Phase Data, (Q) is Quadrature Data, (C) is Carrier, (G) is Gain of the system, (D) is DC Bias, and Φ is the phase of the system:

$$I(t) = G\cos(\omega t + \phi) + D$$
$$Q(t) = G\cos(\omega t + 90°) \qquad \text{[Equation II-5]}$$
$$C(t) = \cos(\omega_C t)$$

Multiplying "I" and "Q" by the carrier and adding the result:

$$RF(t) = G\cos(\omega t + \phi)\cos(\omega_C t) + D\cos(\omega_C t) - \sin(\omega_C t)(\cos(\omega t + 90°)) \quad \text{[Equation II-6]}$$

Note from the above equation that if the DC component value was zero the carrier component would also fall to zero. [11] Figure 1-7 shows an example of an IQ modulator and transmitter chain. A baseband signal on the left passes through the system

and gets converted to a digital signal, encoded to both an “I” and “Q” component. The signal is mixed back up to RF for transmission with data on the carrier frequency as both the “I” and the “Q”.

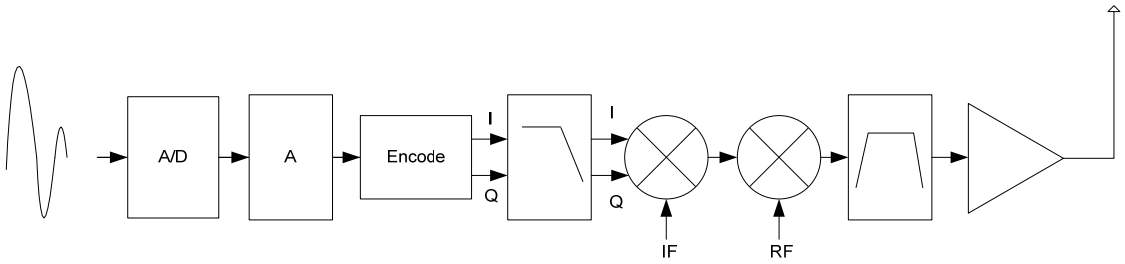

Figure 1-7 IQ Modulator and Transmitter Chain

2 Current Practices

The problems that occur in crystal oscillators under vibration are well known in the industry. Since this is a known problem there are several different solutions already in practice. Two of the most widely used solutions to the problem are vibration isolators and open loop vibration cancellation.

2.1 Vibration Isolators

The most commonly used design technique involves adding a mechanical vibration isolator to the system. This allows the vibration on the oscillator itself to be reduced while the entire system is still under a much higher level of vibration.

Vibration isolation systems are only effective in reducing the level of vibration at vibration frequencies above the system's resonant frequency. There is little effect of the isolator below the resonant frequency. This means that in some situations a vibration isolator could make the system worse than it was before. This is rarely a problem, though, since most isolation systems will have a low resonance frequency well below that of the printed circuit board (PCB) and crystal. At the frequencies above the PCB board resonance the mechanical vibration is greatly attenuated. Figure 2-1 shows an example of the vibration isolation of a particular system based on the resonant frequency. This shows the importance of a low designed resonant frequency of the system compared to the oscillators frequency output.

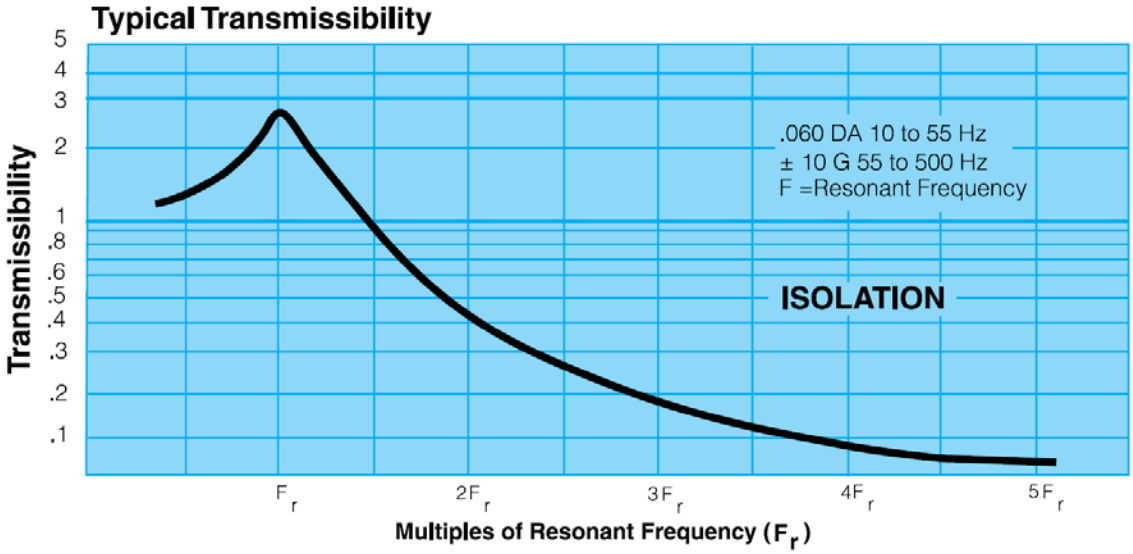

Figure 2-1 Vibration Isolation Based on Resonant Frequency [12]

The design challenge for vibration isolators is attaining a low resonance frequency required with the small size of current mount components. In order to accomplish this, additional mass is needed for the system, requiring additional space. Additional space would be required for mechanical design requirements as well, such as cable tie downs for the added mass.

Figure 2-2 shows the benefits of adding a vibration isolation system. These graphs show the vibration seen by the system with and without a particular vibration system added when excited by a shock of vibration. With the vibration isolator added, the shock is greatly reduced.

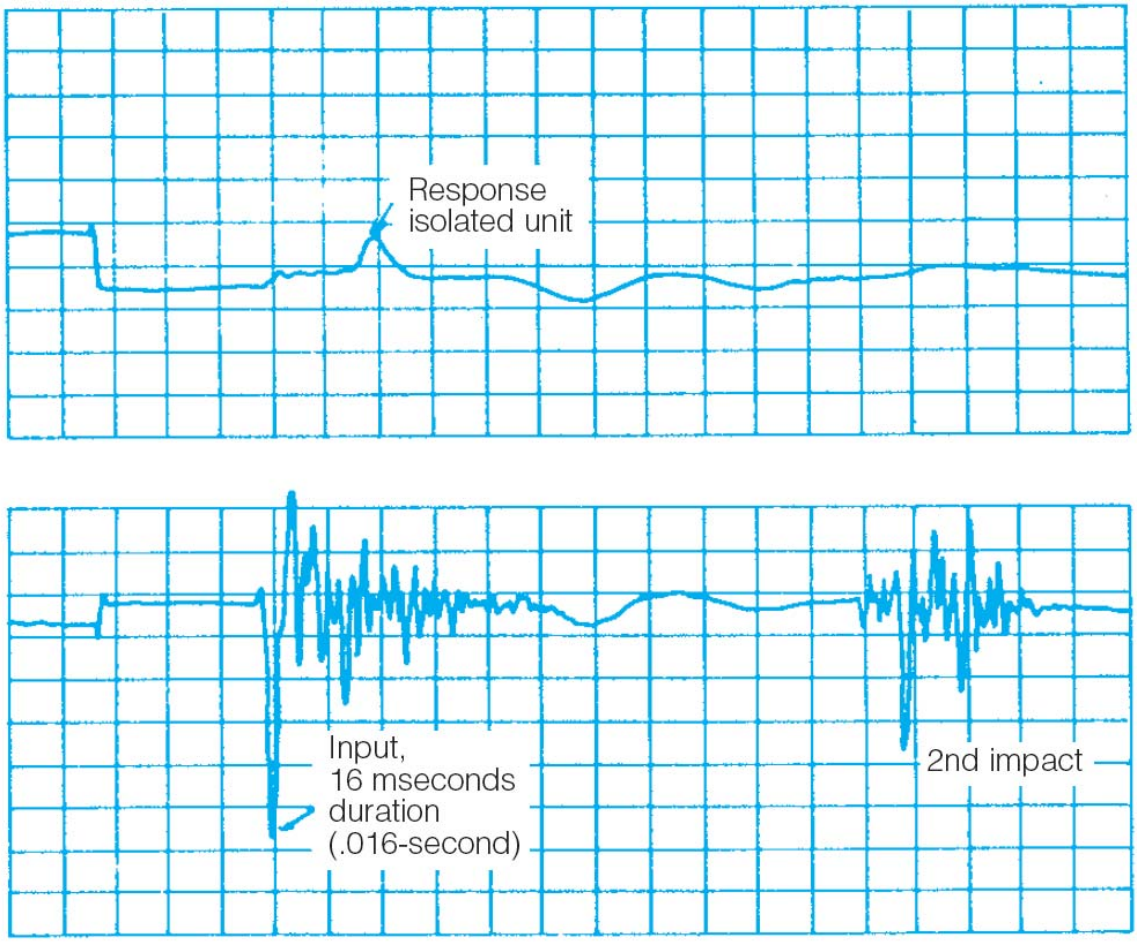

Figure 2-2 Response to shock with [top] and without [bottom] a mechanical vibration isolation system [12]

The vibration isolation system also adds concerns over temperature requirements. The mass plate may react to the temperature by changing stiffness. This change would cause the vibration effect on the crystal to change at different temperatures. This fluctuation makes design stability more difficult.

The non-linearity of a particular material under vibration can be taken advantage of by using it as the mass plate. This way the system can become stiffer at the deflection extremes. To allow this there needs to be extra space added to the system to allow the mount significant room to stretch with temperature.

One example of a vibration isolator used in the industry is the "Circular Arch Series" by Aeroflex International, Inc, shown in Figure 2-3. The benefits of this particular design are that it provides consistent performance over temperature and time as well as producing omni-directional isolation. [6]

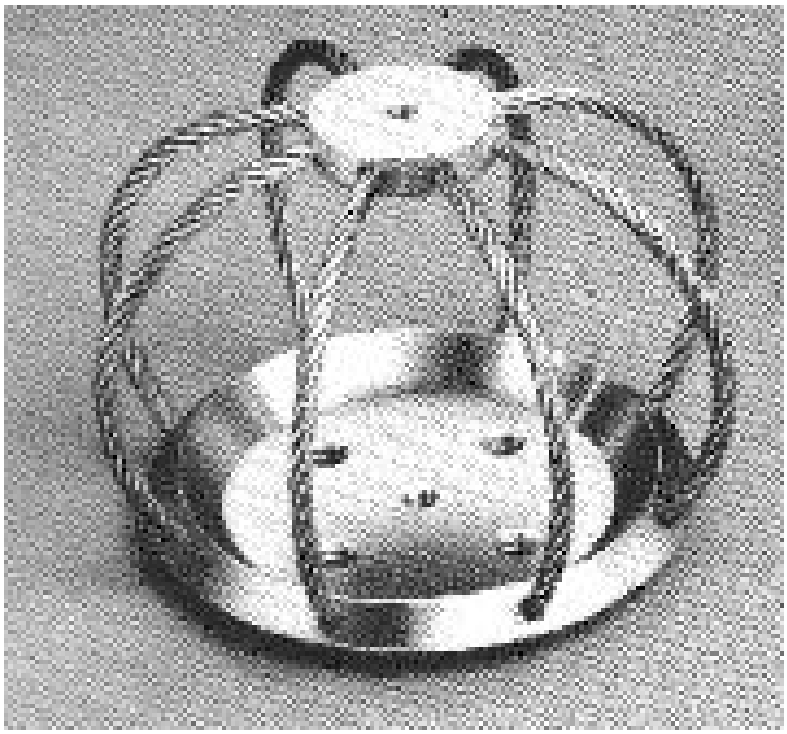

Figure 2-3 Circular Arch Series Vibration Isolator [6]

Despite all the benefits of reducing vibration on the crystal oscillators, there are some impracticalities of the vibration isolator. Not all systems that use a crystal oscillator have the ability to accommodate the weight, size and shape of the design to fit in the dampener. It would make the system cumbersome and unwieldy.

2.2 Polarization-Effect Tuning

An alternative to vibration isolator systems is that of the "polarization-effect tuning" method [13]. The method consists of sensing the acceleration with an accelerometer, amplifying and phase inverting the sensing signal, then feeding that information back into the oscillator. The use of this method has shown some historical

improvements of phase noise. Initial results of this method yielded the results showing Figure 2-4 and Figure 2-5. Figure 2-4 shows the phase noise of the oscillator without any vibration reduction techniques. The lower line shows the oscillator under quiescent conditions, while the higher line shows the same oscillator under random vibration. This shows an increase of 30 dBc of the oscillator under random vibration conditions. Figure 2-5 shows the oscillator under vibration without any phase noise mitigation technique, then again with the oscillator having the polarization-effect tuning method used as its phase noise mitigation technique. Early attempts at this system show a maximum of 30 dB improvement in phase noise under the polarization-effect tuning method, but limited improvement over most offset frequencies.

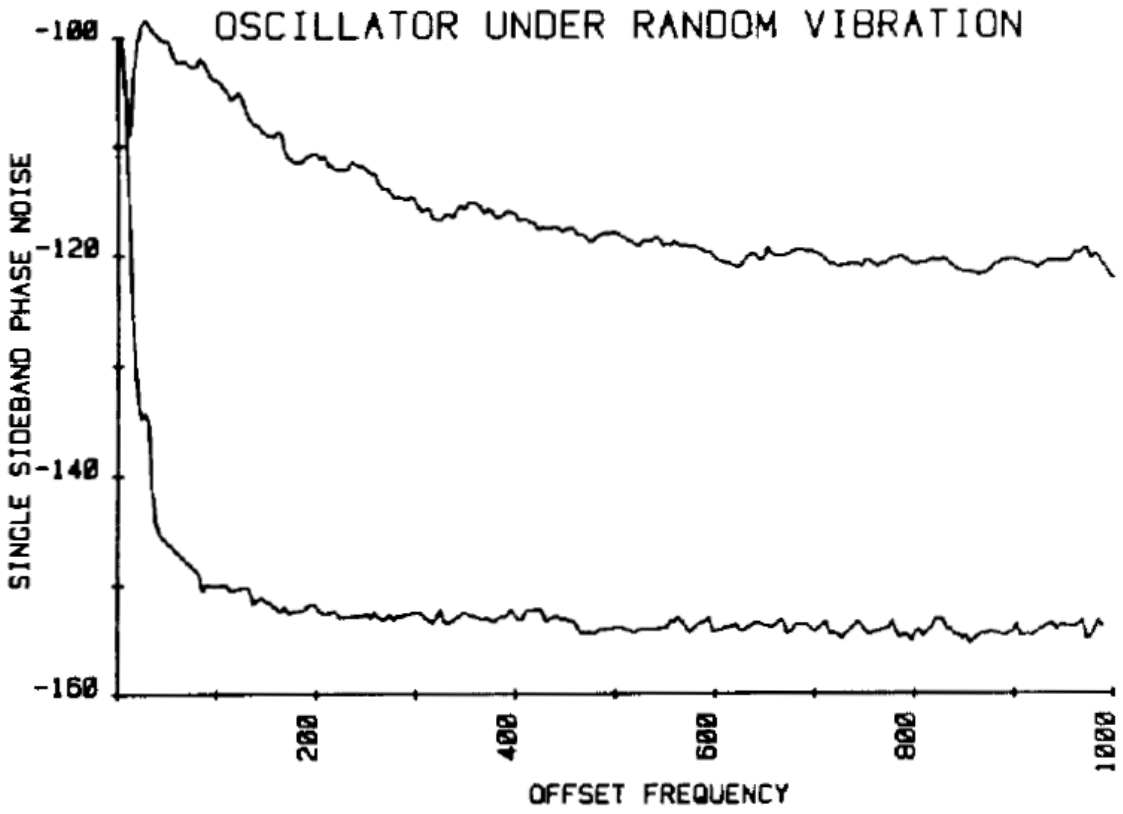

Figure 2-4 Oscillator under Random Vibration [13]

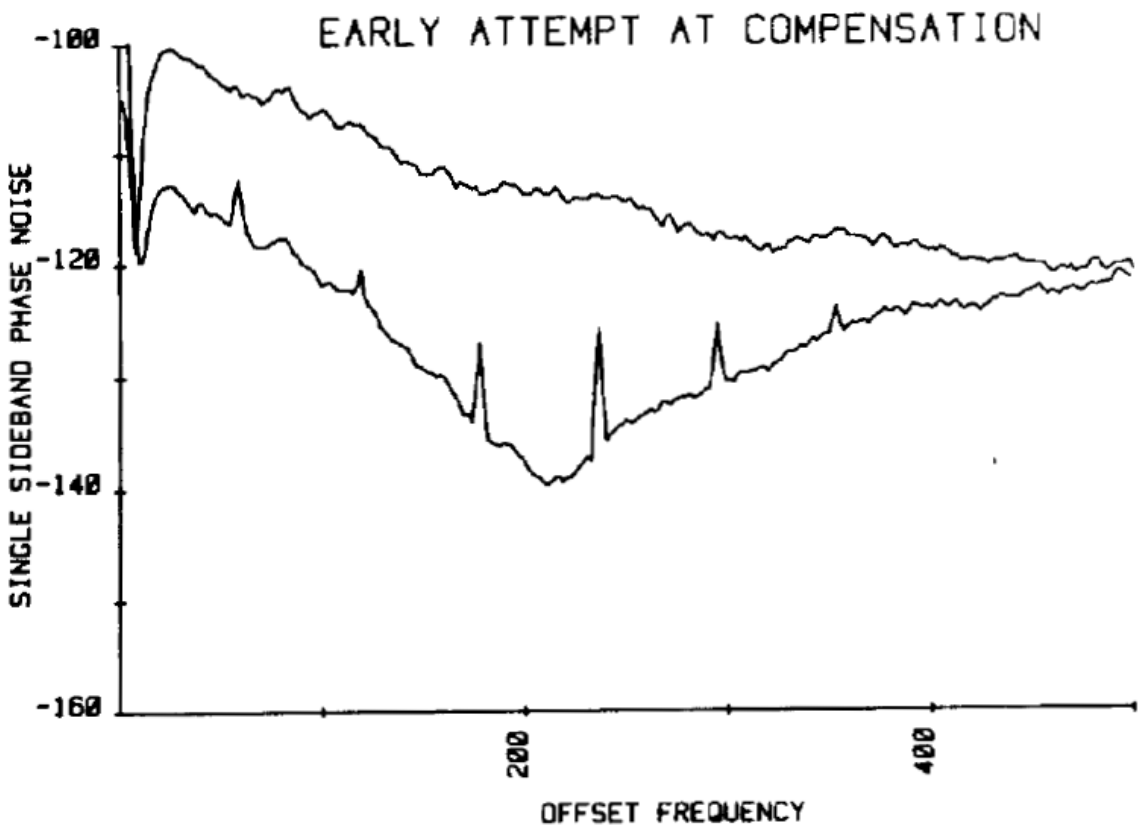

Figure 2-5 Polarization-Effect Tuning Method of Phase Noise reduction [13]

Early attempts at compensation were limited by the technology at the time. The speed of the accelerometer was slower than it is now and the charge amplifiers didn't take into account phase shifts resulting from their distance from the oscillator. With those types of changes in mind, Figure 2-6 shows an example of a schematic. This is a simplified version of the schematic showing the set up required for the compensation. [13]

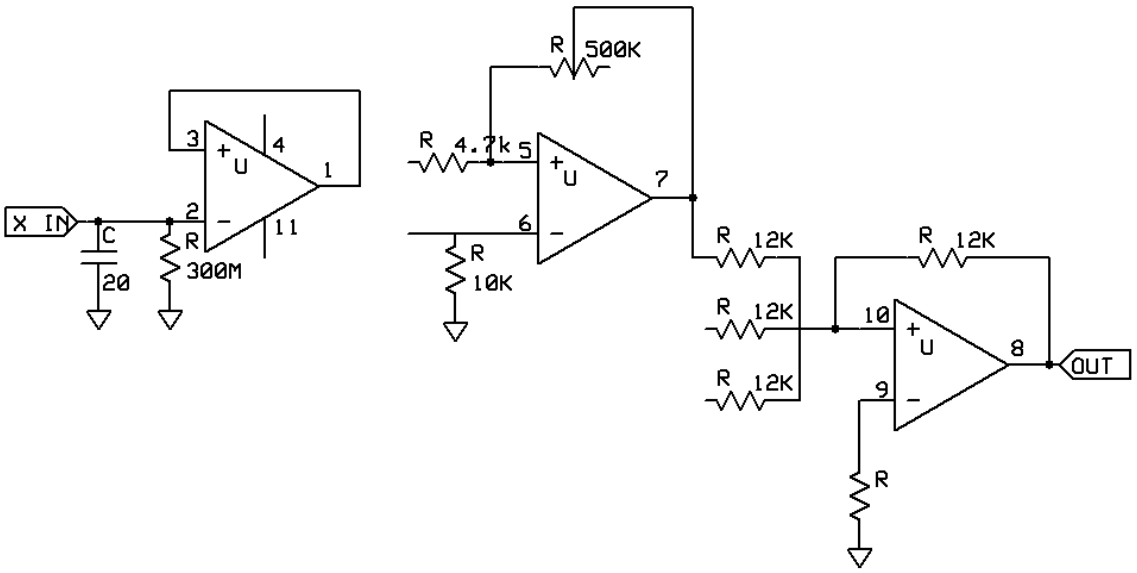

Figure 2-6 Schematic of Polarization-Effect Tuning Phase Noise Mitigation

In order for the sine waves of the vibration to cancel, two main contributing factors are required, the phase and the amplitude.

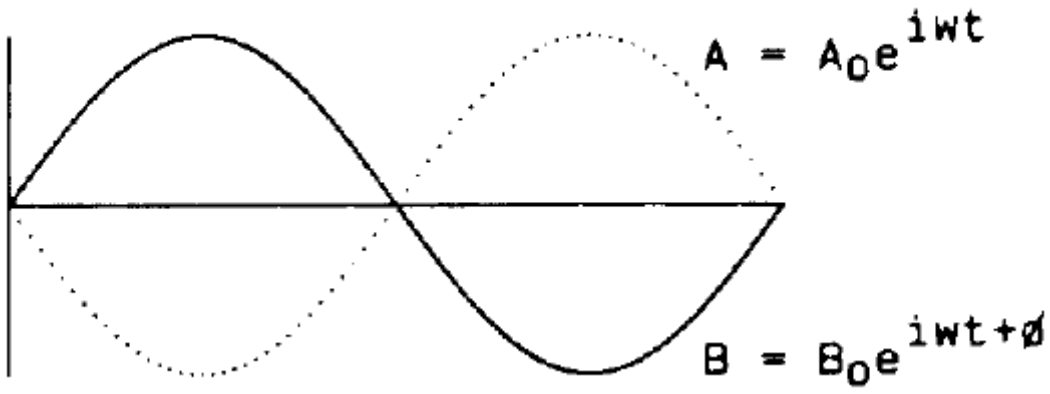

Figure 2-7 Sine Wave Cancellation Model [13]

The intensity of resultant is:

$$S^2 = A_O^2 + B_O^2 + 2A_O B_O \cos(\phi) \qquad \text{[Equation III-1]}$$

The ratio of intensities is:

$$R = \frac{S^2}{A_O^2} \qquad \text{[Equation III-2]}$$

Letting A_O=1 then it follows that:

$$10\log(R) = 10\log(1 + B_O^2 + 2B_O\cos(\phi)) \qquad \text{[Equation III-3]}$$

Equation III-3 needs to be considered to maximize circuit design. The speed of response of the accelerometer will affect the phase difference between the vibration and the cancellation signal. The distance of the signal between components is also important: as the distance increases, the phase and amplitude change could vary. A minimal distance design is desirable because of this. Figure 2-8 shows the impact of a shift in either amplitude or phase away from the desired vibration frequency on the attenuation of that frequency.

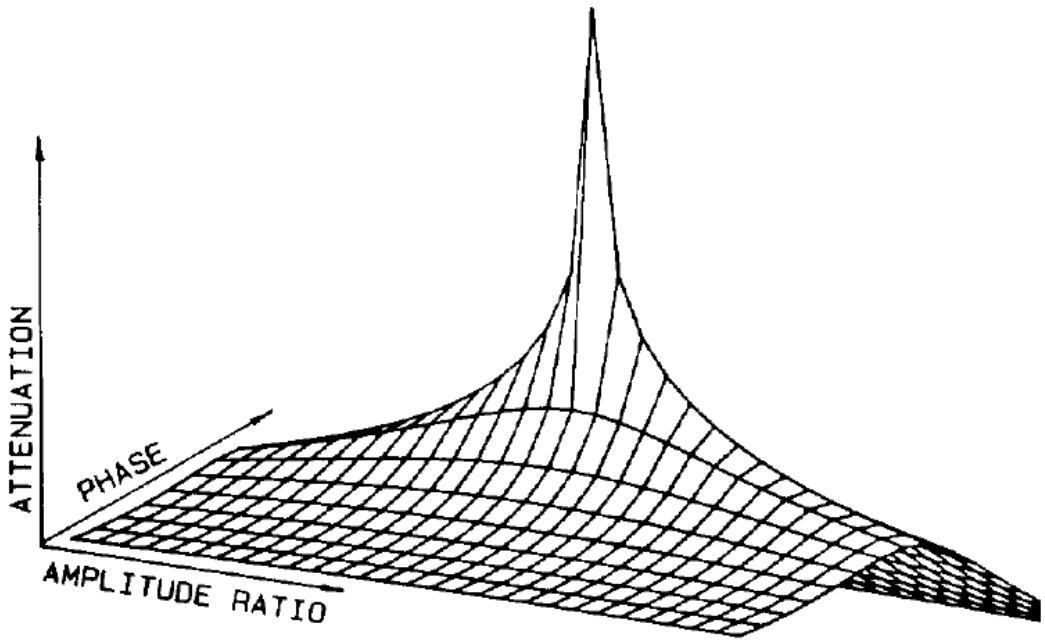

Figure 2-8 Sensitivity Surface of Attenuation [13]

Based upon this information, alternate circuits were designed to take advantage of higher speed accelerometers and shorter signal length. [13] Figure 2-9 and Figure 2-10 show the close in and full range phase noise suppression using the polarization technique. From these results the advances and advantages to a design such as this one can be seen. Figure 2-9 shows the oscillator circuit under vibration with the modified polarization tuning circuit compared to the oscillator under random vibration without any vibration correction. This shows a more uniform improvement over the original polarization tuning circuit of over 30 dB improvement to 250 Hz offset frequency. Figure 2-10 shows the same as Figure 2-9, but over a wider range of offset frequencies. This shows that this correction benefit is more limited at higher offset frequencies. Compared to Figure 2-1 it shows that at lower offset frequencies the polarization tuning method has benefits over that of the mechanical isolator, but as the offset frequency increases the mechanical isolator provides better performance.

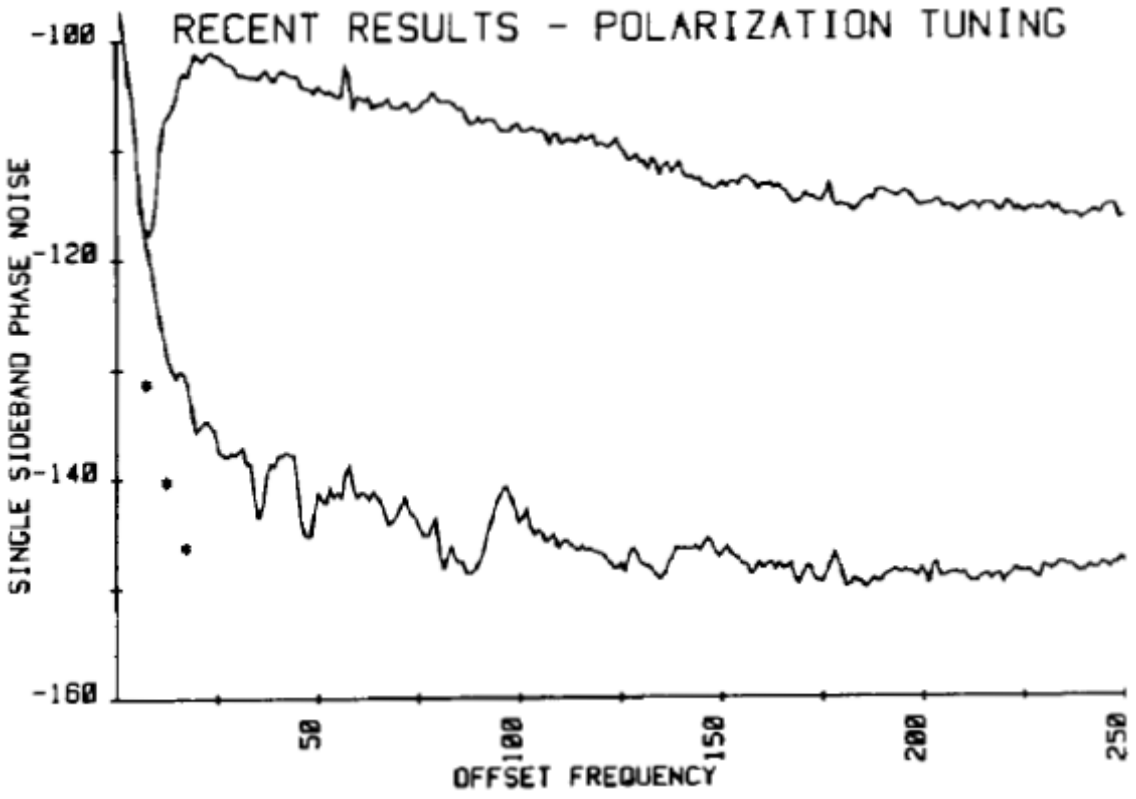

Figure 2-9 Polarization Tuning Close In Phase Noise Results [13]

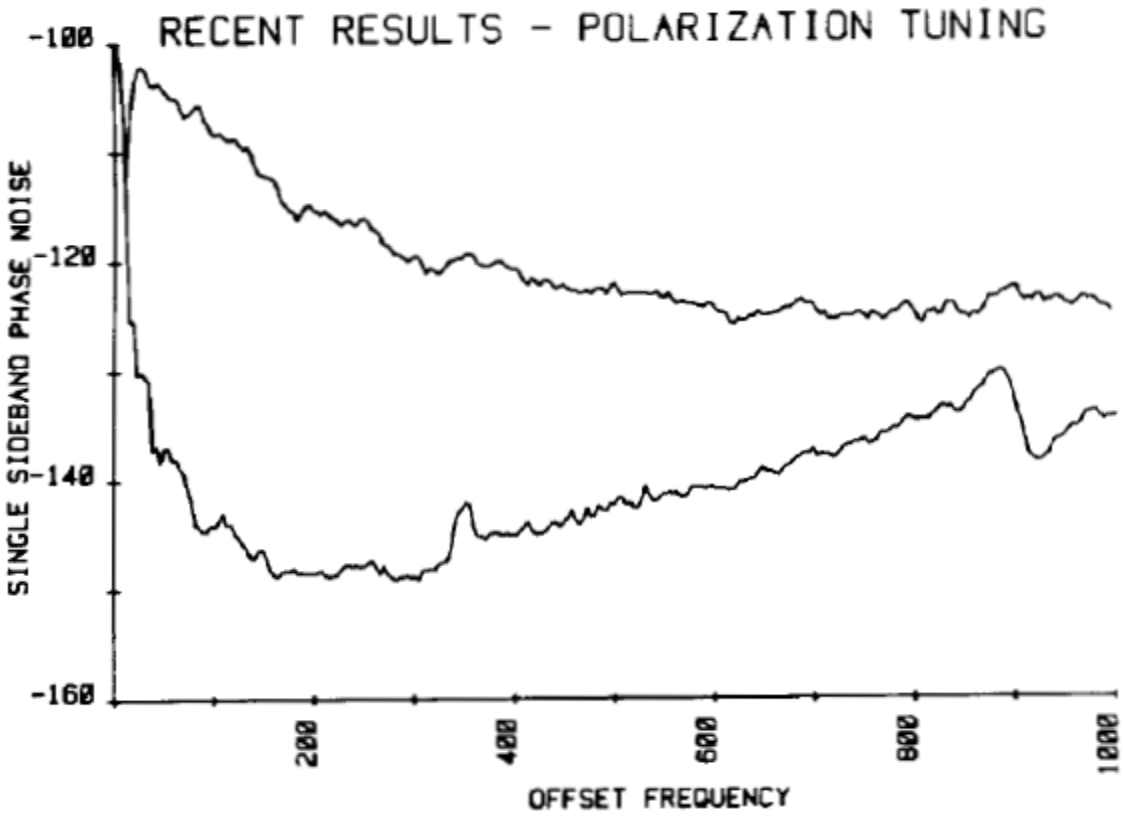

Figure 2-10 Polarization Tuning Full Range Phase Noise Results [13]

When ever you add components to a circuit board this adds complexity to the circuit design. With added complexity always comes the added risk of error and performance degradation. The affect of the added components to the system should be considered not only under vibration, but in stable conditions as well. It can be seen in Figure 2-11 that the added circuitry for polarization tuning correction has affected the overall system very little.

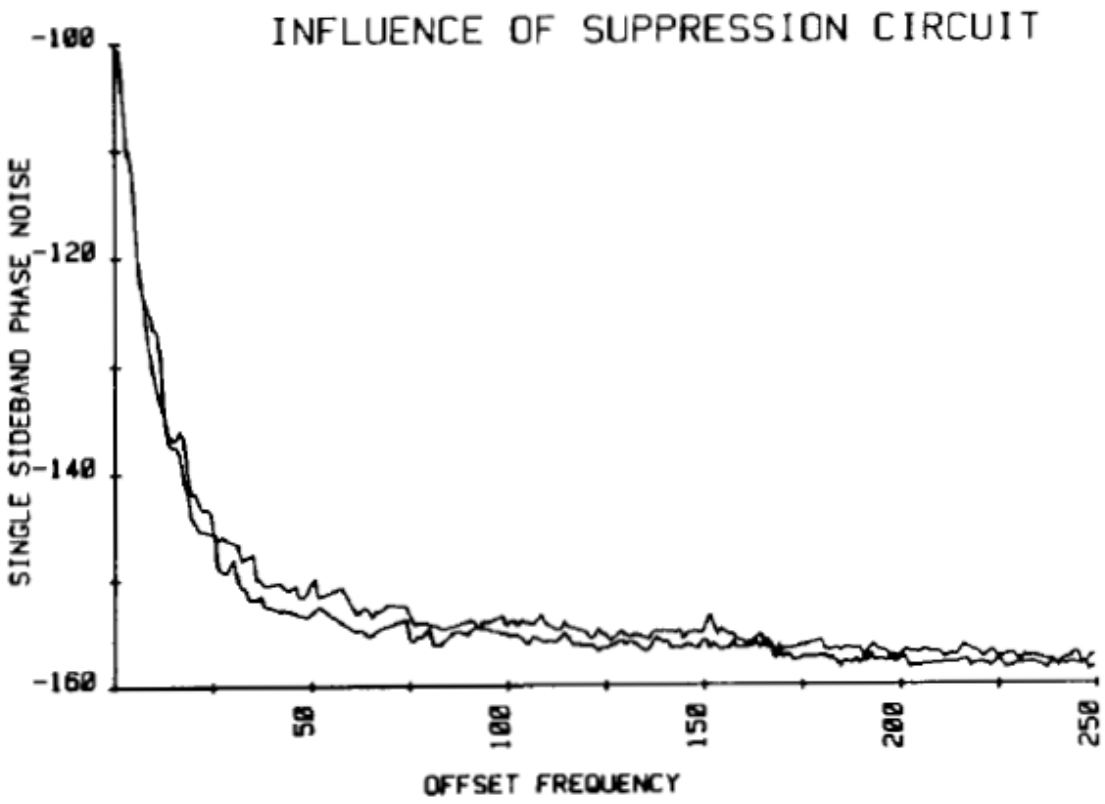

Figure 2-11 Without Vibration Influence of Suppression Circuit [13]

Any design that has added circuitry does come with drawbacks. It increases circuit complexity and design time for engineering. This might lead some projects to prefer the vibration isolator system to a suppression circuit. The polarization tuning suppression circuit design has a suppression rollup at 300 Hz, which is very undesirable as well. Another concern with this current practice is that it doesn't take into account the output of the crystal oscillator as feed back is added and changed. This can cause instability and causes a lack of ability to respond to changes in the oscillator.

3 Analysis and Results

Based on the polarization tuning design it can be concluded that there has been solid advancement in reducing size in the design while maintaining the required phase noise for the system. This still leaves some aspects of design lacking, however, as more needs to be done to incorporate a feedback system to measure the current phase noise output of the oscillator and increase or decrease the needed change based on that. Many design efforts need to be taken into account to meet this goal. With many oscillators having voltage control to correct the frequency the phase noise could be controlled through this pin. A system would need to be put into place to analyze the phase noise of the oscillator and regulate it using the control voltage pin. The phase noise of the system would need to be integrated and measured. This would all need to be mixed together to include the necessary information into one control voltage to feedback.

3.1 Circuit Design

Using the research of Rosati [13], it can be concluded that taking advantage of the oscillator's frequency control allows reduction of phase noise. By reducing the delta of the frequency, the overall phase noise is reduced and adequately cancelled. Rosati does this by canceling the f_v which effectively reduces the affect on the crystal due to vibration. In order to accommodate the voltage control of the oscillator, a system would need to be devised to create a feedback loop to the oscillator.

The signal is an IQ modulation chain is shown in 1.5 to be a vector. This vector can be broken down into X and Y components. The accelerometer output and the carrier phase noise are mixed together using a MOSFET, resulting in the following X and Y components. The accelerometer output speed is represented as ω_a, ϕ represents the phase noise of the system added by vibration, ω_c is the output speed of the integrator, V_x is the voltage at that stage of design on the X channel, and V_y is the voltage at that stage of design on the Y channel.

$$V_x = |X|\cos(\omega_a t + \phi)\cos(\omega_c t) \quad \text{[Equation IV-1]}$$

$$V_y = |Y|\cos(\omega_a t + \phi)\sin(\omega_c t) \quad \text{[Equation IV-2]}$$

Equation IV-2 is the same as Equation IV-1 except for the 90 degree phase shift that comes with the change in axis of vibration, therefore sin is used instead of cos. Multiplying out Equations IV-1 and IV-2 results in the following equations.

$$V_x = |X|\cos((\omega_a + \omega_c)t + \phi) + \cos(\Delta\omega t + \phi) \quad \text{[Equation IV-3]}$$

$$V_y = |Y|\sin((\omega_a + \omega_c)t + \phi) + \sin(\Delta\omega t + \phi) \quad \text{[Equation IV-4]}$$

A low pass filter is used to take out the high frequency component of $\omega_a+\omega_c$. This leaves the equation with just the delta frequency component and the phase noise. The X and Y components are then summed together to get the following result.

$$\sum = |A|\cos(\Delta\omega t) + |B|\sin(\Delta\omega t) \quad \text{[Equation IV-5]}$$

$$A = |X|\cos(\phi) + j|Y|\sin(\phi) \quad \text{[Equation IV-6]}$$

$$B = \cos(\phi) - j\sin(\phi) \quad \text{[Equation IV-7]}$$

As the feed back corrects itself the cosine term of Equation IV-5 will approach 1 and the sinusoidal term will approach 0. This will result in a feedback value of A which will be approximately ϕ. Thus giving a feedback system that gives the phase noise result back into the oscillator to allow correction based on the vibration.

It can be seen from the block diagram, in Figure 3-1, that the output of the oscillator is coupled into a feedback circuit. The feedback circuit consists of an integrator block combining with the X and Y axis of the accelerometer. This then creates the channels similar to that of the "I" and "Q" channels of an IQ mixing scheme. These channels are then recombined to create a final control voltage which is fed back into crystal oscillator to create a closed loop design.

The benefit of this design over previous designs is the ability to recognize changes in both major axes of vibration, as well as dealing with the tilt effect on the crystal. Another major benefit is that as the phase noise improves, despite the level of vibration, this system has the ability to increase or decrease the rate of change of the voltage control line. This adds another dimension of controllability to assure under all conditions the phase noise is minimized. As the delta in the phase noise integrator increases, the increased voltage forces the control voltage to increase to minimize the phase noise back to an ideal level.

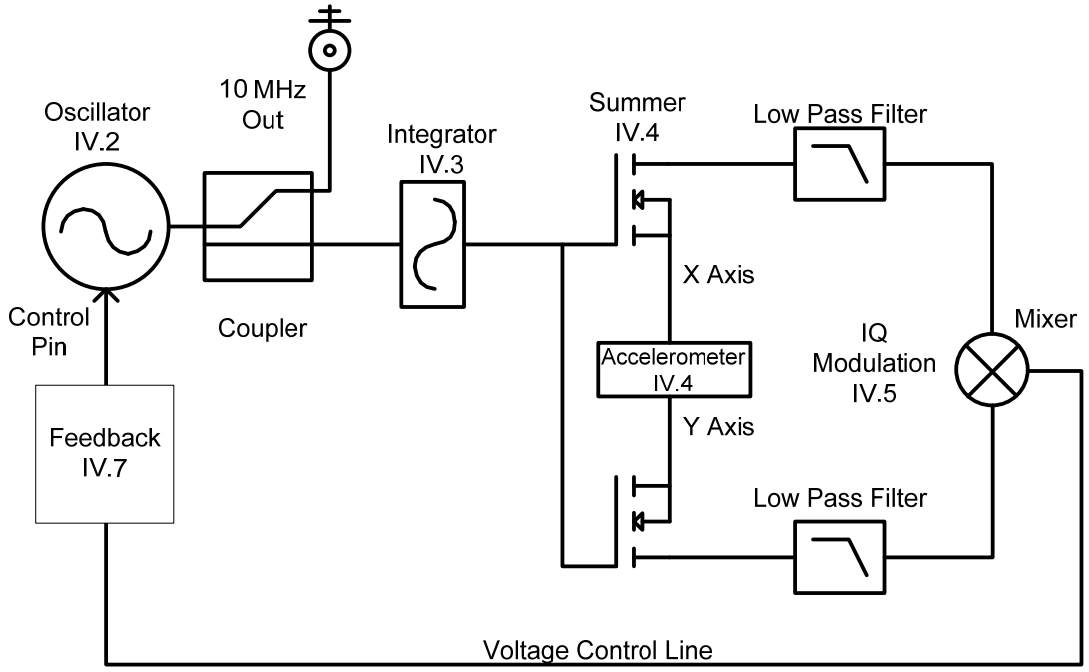

Figure 3-1 Phase Noise Reduction Circuit Block Diagram

Based on the block diagram, the system was broken down into six major circuits: oscillator, integrator, accelerometer, summer, IQ modulator, and feedback. These six circuits were designed and tested individually as parts to be recombined into the final circuit after their completion. Each circuits design is discussed in the sections that follow. Power consumption wasn't a design concern for this project. The design wasn't intended to be used on battery applications, but could be modified in design to work under those conditions.

The circuits described in the sections that follow were designed as a team effort at Rockwell Collins. I was the primary designer of all circuits described, but Henry Eniola and Mark Yu had oversight of the entire project. They were available to aid in design and answer questions I had. Lab technicians were available to assist with all tests and circuit build up.

3.2 Oscillator

Phase Noise increases as the frequency of a crystal oscillator shifts due to vibration. This fact leads to the notion that limiting the frequency shift of the crystal limits the phase noise increase of the oscillator. This is the concept used by Rosati [13].

In order to accomplish this, the crystal oscillator needs to be designed or chosen with the capability of frequency control. Other design considerations for the oscillator in this project were the general phase noise, the size of the unit, tilt sensitivity, and the frequency of oscillation. For this project a 10 MHz sine wave oscillator was required. For these reasons a CTS electronic components oscillator PN1960027 was chosen.

The CTS electronic components oscillator is characterized to have phase noise listed in Table 1. This is also compared to measured results for both quiescent and under vibration. The data sheet level is under quiescent conditions.

Table 1 Oscillator Phase Noise

Offset	Data Sheet Level [14]	Quiescent Level Measured	Vibration Level Measured
10 Hz	≤-110 dBc/Hz	-86 dBc/Hz	-80 dBc/Hz
100 Hz	≤-130 dBc/Hz	-108 dBc/Hz	-89 dBc/Hz
1 KHz	≤-140 dBc/Hz	-112 dBc/Hz	-96 dBc/Hz
10 KHz	≤-145 dBc/Hz	-118 dBc/Hz	-114 dBc/Hz

Phase noise was measured using an Agilent E5052 phase noise analyzer. The measured phase noise and under vibration measured phase noise, from Table 1, is shown in Figure 3-2 below. Figure 3-2 shows the performance of the crystal oscillator while under vibration. The green and purple signals represent the performance with vibration and the blue represents the quiescent state. The vibration level applied was a sweep from 10 Hz to 10 kHz at 500 mV applied to the vibration table. The g level varied slightly based on frequency, but was approximately 1.0 g per V applied.

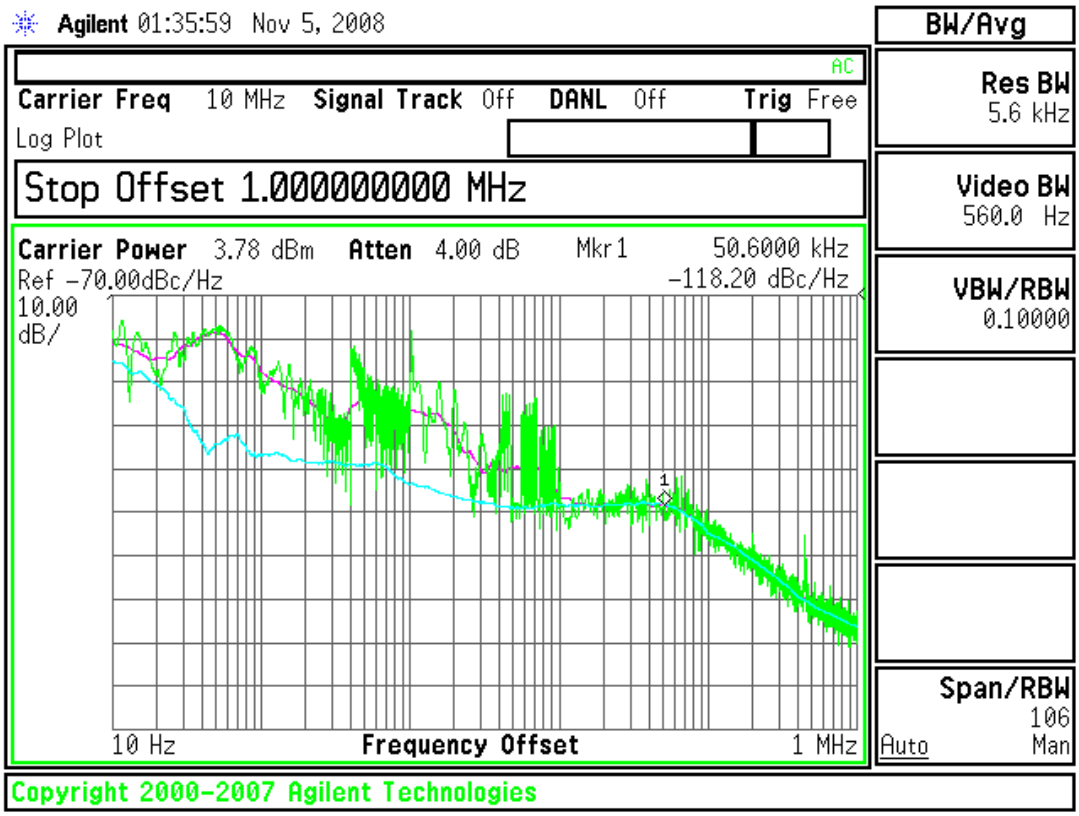

Figure 3-2 Crystal Oscillator Performance Under Vibration

Based on this, it can be appreciated that there is a significant degradation of the crystal under vibration. The degradation seen at low frequencies can be upwards of 20 dB at low levels of vibration. The vibration region as a whole experienced nearly 10 dB over the span of 10 Hz to 10 KHz.

This leads to the requirement of frequency control to correct phase noise. The voltage control line is rated to 5 VDC according to Table 2 below.

Table 2 Electronic Frequency Adjustment [14]

Control Voltage	0 to + 5.0V
Slope	Positive
Range	≥ ±0.55 ppm from 10 MHz
Input Impedance:	≥ 50 KΩ

The performance ability of the voltage control line is demonstrated in Figure 3-3. In this figure the blue line represents the frequency of the oscillator with the control pin at 0.3 VDC, and the green line demonstrates it with the control voltage pin grounded. The phase noise of the lines again shows the performance of the oscillator with and without vibration. The green line has vibration applied at the same level as specified above; the blue line is at the quiescent condition. This was done for another baseline measurement.

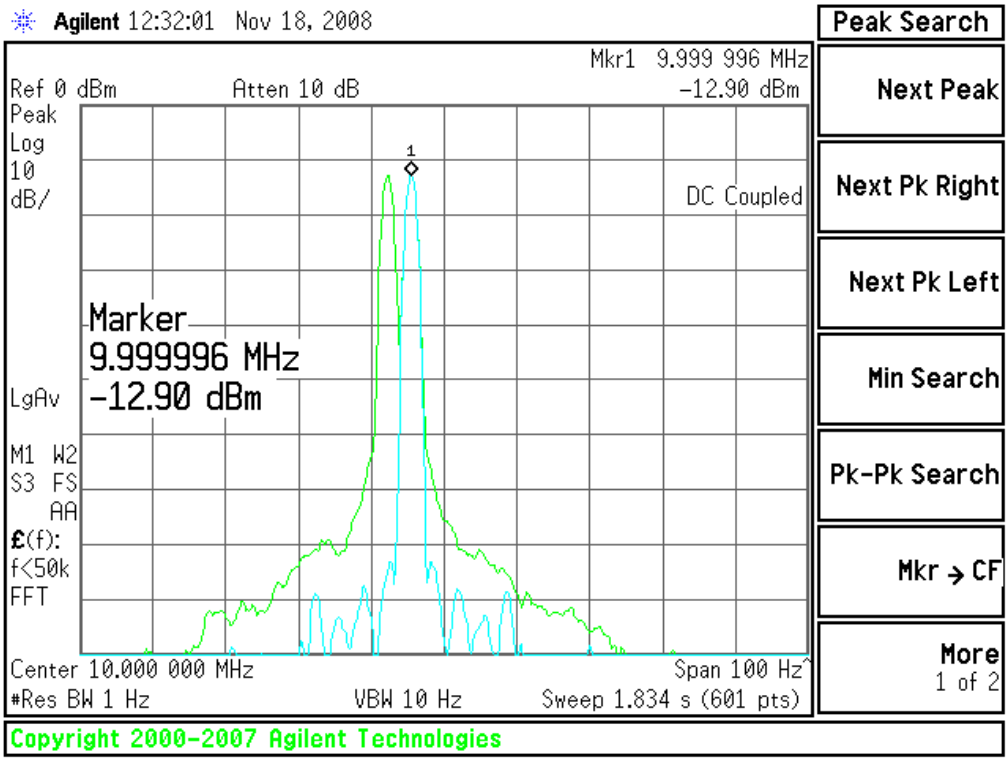

Figure 3-3 Frequency Shift with Voltage Control Pin

This shows that this oscillator chosen has adequate ability for frequency control as well as significant room for improvement in phase noise areas. This made it an acceptable choice for the design. However, the ability to simulate this crystal's phase noise performance needed to be addressed.

In order to simulate the phase noise performance in Agilent Advanced Design System (ADS) licensed to Rockwell Collins, a Phase Modulation (PM) demodulation block needed to be added to the system. Any SPICE like program could be used for all simulations used, ADS was chosen for the ability to add parasitics and noise for future design considerations. This yielded the circuit diagram shown in Figure 3-4. For this simulation an ideal source was used with a phase noise input P=dbmtow(10). The added phase noise represents an approximate level of vibration as observed in the lab tests described above.

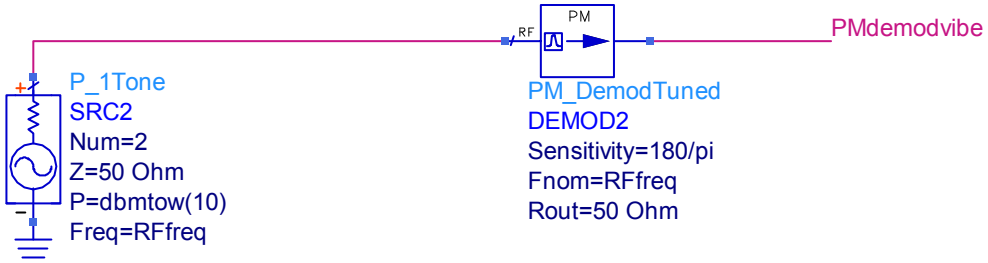

Figure 3-4 ADS Oscillator Simulation

Simulation of that circuit gave the following phase noise results seen in Figure 3-5. In these results the blue line shows the oscillator's simulated performance under a higher level of vibration while the red line shows the vendors data sheet representation of the oscillator's phase noise performance. This simulation's output was then used as the input for other circuits when they were simulated using ADS.

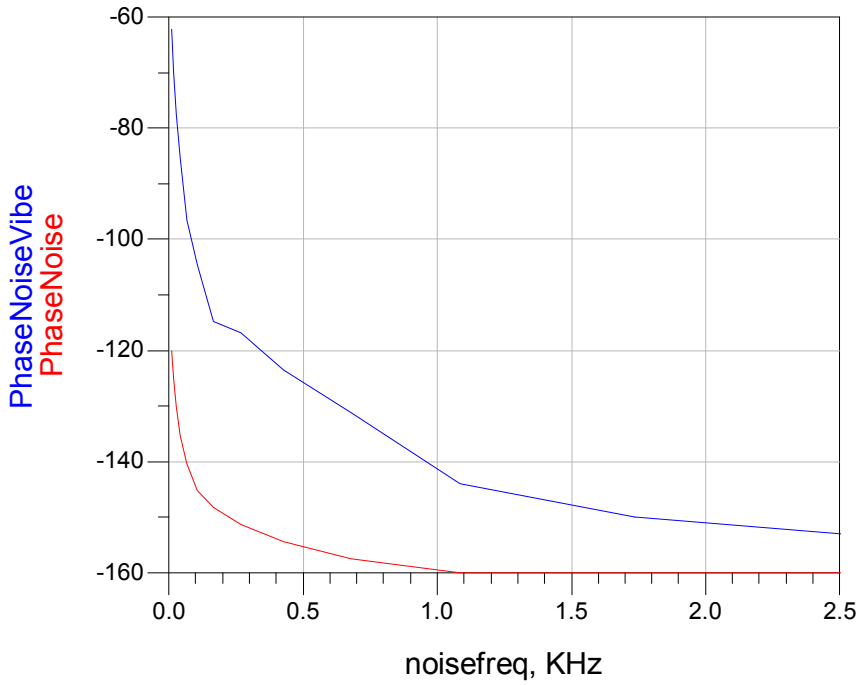

Figure 3-5 ADS Oscillator Simulation Results

On the output of the oscillator circuit is a RF coupler used to split the signal between the output and the control loop. The directional coupler chosen was the mini circuits DBTC-12-4. According to the vendors data sheet for this component it is rated between 5 and 1000 MHz. The insertion loss from the input to the output of the coupler is typically 0.79 dB for 10 MHz. At the 10 MHz band, the input to the coupled output insertion loss is typically 11.96 dB. [15]

The coupled output has an inherent insertion loss, because of this that output was chosen to be the output of the system. A 10 dB amp is used to get the loss down to approximately 1.96 dB. The output port of the coupler is used for the feedback loop because of its low insertion loss and flat spectrum, and there are no amplifiers needed before the integrator circuitry.

3.3 Integrator Circuit

The integrator circuitry is used to create a DC voltage level induced by the phase noise of the oscillator. This voltage will then be used as part of the feedback control loop. The integrator circuit is made up of a simple RC design similar to a Low Pass filter. This design was tuned to be at the end of the frequency range of phase noise required, which was 2 kHz. A cutoff frequency of 2 kHz was chosen because further down the design chain the phase noise less than 2 kHz had the least margin. Decreasing the phase noise under the 2 kHz in particular would enhance the system margin. This passive design can be updated with an operational amplifier to better control the voltage output of the circuit and accentuate the delta in the voltage based on phase noise changes.

The design of an Integrator Circuit is based on an RC low pass filter. Based on the time constant of the capacitor in the frequency domain, the oscillating voltage applied can be integrated. Since there is a concern with the oscillation noise from 10 Hz to 2 kHz this gives a RC circuit tuned to 2 kHz.

$$V_{in} = \sqrt{R^2 + \left(\frac{1}{\omega C}\right)^2}$$

$$\omega C >> \frac{1}{R}$$

$$V_{in} \cong IR \qquad \text{[Equation IV-8]}$$

$$v_{out} = v_C = \frac{q}{C} = \frac{1}{C}\int i \cdot dt \cong \frac{1}{C}\int \frac{v_{in}}{R} \cdot dt$$

$$v_{out} \cong \frac{1}{RC}\int v_{in} \cdot dt$$

The above equations give the theory behind the integrator coming up with the voltage output as the integration of the voltage in [16]. The choice of R and C values for this circuit were based on the following equation.

$$f_c = \frac{1}{2\pi RC} \qquad \text{[Equation IV-9]}$$

The initial design option took f_c to be 2.5 kHz. This choice was based on the 2 kHz frequency bandwidth under vibration, since no significant roll off was desired before 2 kHz. In order to compensate this, a higher frequency was chosen. The output of the coupler is a 50 ohm system so the system needs to be matched to 50 ohm, giving the R value of 25.

$$2500 = \frac{1}{2\pi 25C}$$
$$C = 2.55\mu F$$

Using this value the following circuit was put into ADS. For this simulation an ideal capacitor was used without accounting for the parasitic effects that would occur with a commercial off the shelf component.

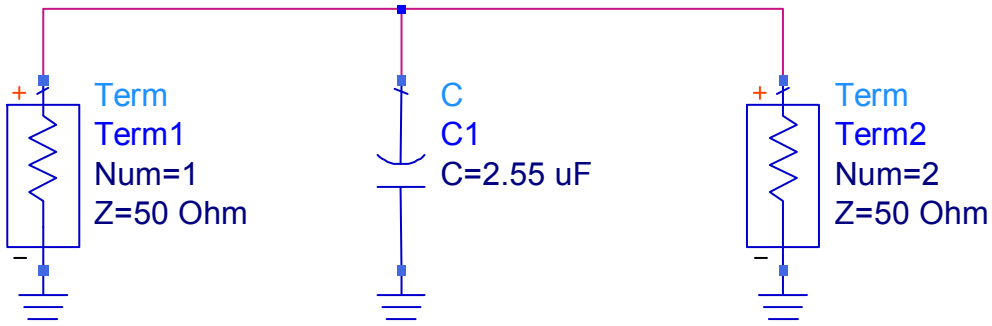

Figure 3-6 Integrator Circuit Design - Simulation

This circuit led to the following performance results of Figure 3-7. The results of the simulation were compared to other results with more stages added in. These other results with multiple stage integrators are not shown. It was decided that a simple one stage integrator circuit would add adequate performance for the region of 10 Hz to 2 kHz despite the 2 dB drop between these sections. The consideration was that adding more poles would add more complexity to the design. Also the highest phase noise change would occur close in to the signal. The close-in insertion loss is required to be less than 1 dB to allow the higher phase noise change to be captured adequately.

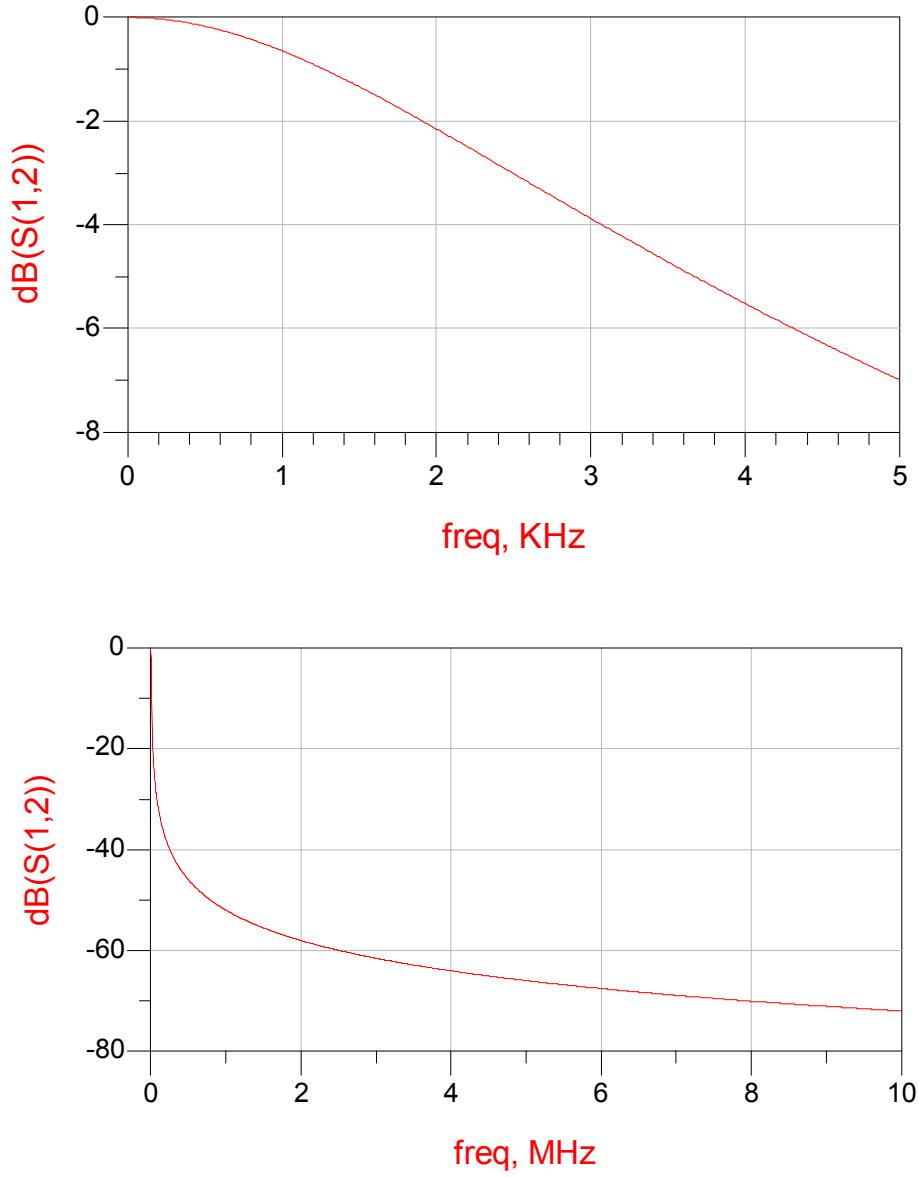

Figure 3-7 Integrator Circuit Design - Simulation Performance Results

Figure 3-7's results show this circuit's frequency range. To adequately show the power as an integrator of phase noise another ADS simulation was set up using the phase

noise input described above. The results are shown in Figure 3-8. It is shown as voltage change (Y axis) vs. the frequency output (X axis). The red line of the graph represents the output of the integrator circuit with the phase noise performance of the oscillator without added vibration noise. The blue line represents the output of the integrator circuit with the phase noise performance of the oscillator with added vibration phase noise. This chart shows that the signal with no vibration signal is 0 volts across the entire frequency range. The signal under vibration has a DC component of 1.1 mV while the rest of the frequency range remains at 0 volts. Based on these results it is considered reasonable to use the above circuit, Figure 3-6, as the phase noise integrator. The important result is that there is a delta between different levels of phase noise. Since this delta is small, a design of active components could be considered.

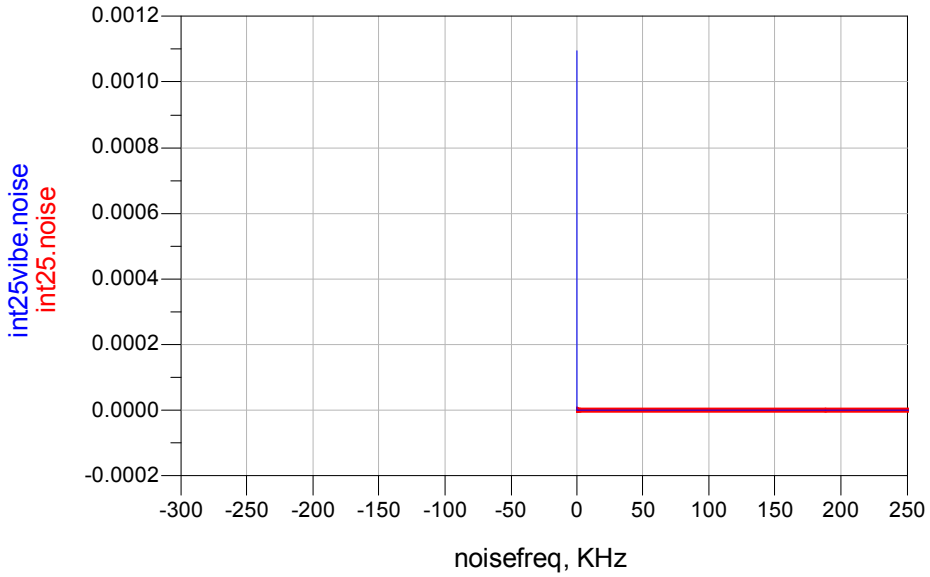

Figure 3-8 Integrator Circuit Design - Simulation Integration Results

As shown in Figure 3-9, it is a simple change from the passive circuit to the active circuit. The equations to choose a value for C remain the same so 2.55 μF can still be used. The only change is that this circuit design allows a gain factor. [17]

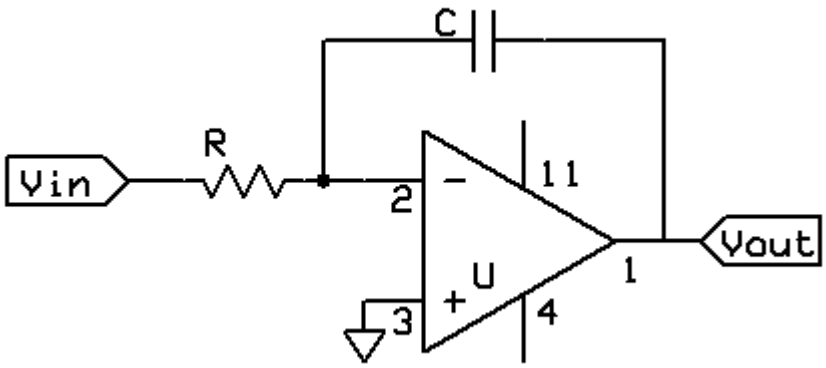

Figure 3-9 Active Integration Circuit Design

A simple test was set up to verify the results of the simulation with the passive components before proceeding. For this test, a 10 MHz oscillator was placed on a vibration table and the signal from that was fed into the circuit shown in Figure 3-10. The output of this was measured with a digital multi-meter and the voltage changes based on vibration were observed.

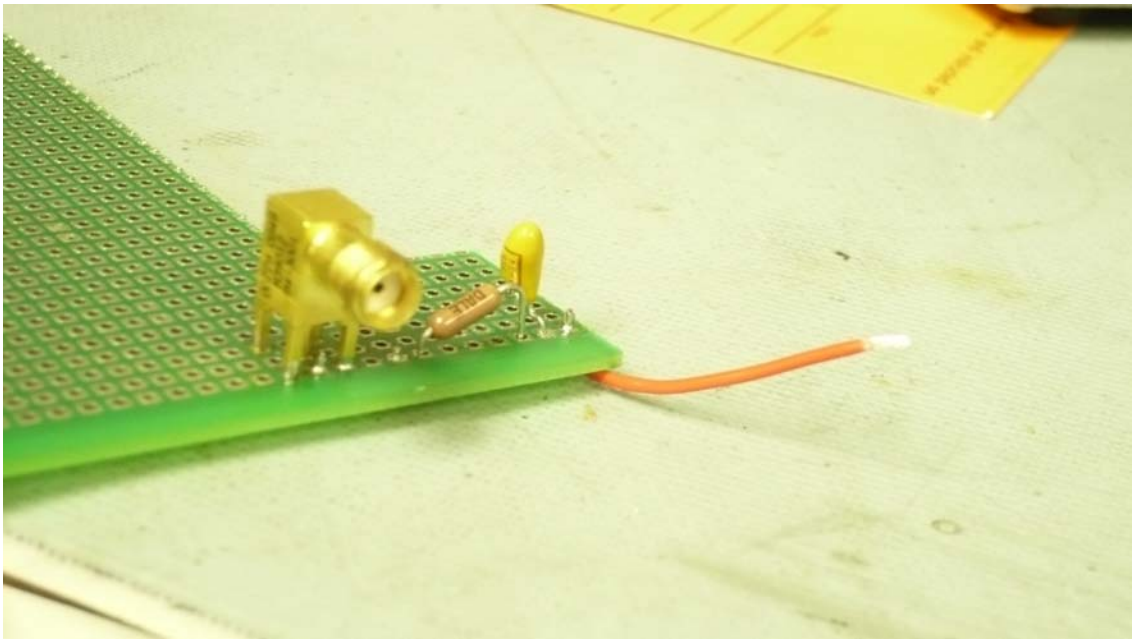

Figure 3-10 Integrator Passive Circuit Test

After the oscillator settled at quiescent conditions the output of the circuit measured 0.01 mV. During a state of low level vibration the measured data was 0.2 mV. The simulation resulted in 1.1 mV instead of the 0.2 mV of the test because the frequency and force of acceleration for the test were at a reduced level. The phase noise integration was creating the voltage change based on vibration as expected.

To increase the gain even more, the circuit was changed from the active version of the filter shown in Figure 3-9 to a passive filter followed by an operational amplifier with adjustable gain.

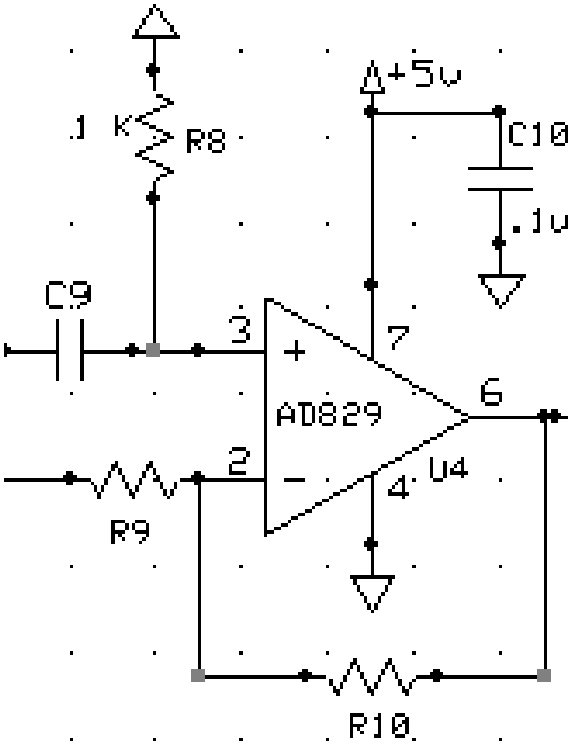

Figure 3-11 Integrator Block Design with Gain

This leads to a gain of the circuit based on R_9 and R_{10}. [18]

$$G = 1 + \frac{R_{10}}{R_9} \quad \text{[Equation IV-10]}$$

For testing this circuit, R_{10} was set to be much less than R_9 making the gain virtually unity. Under these conditions and the same vibration conditions used with the passive circuit test, a 0.5 mV change was found between quiescent and vibratory states. R_9 and R_{10} could then be chosen to get the ideal conditions for the feedback loop.

3.4 Accelerometer Circuit

The accelerometer block is used to measure the vibration on the crystal. It is imperative to create the design with close proximity to the crystal oscillator package. This is because different sections of the same printed circuit board may experience different levels of vibration. The board's axis may also experience shifts based on the intended use. For example, a board mounted inside an airplane wouldn't be parallel with the ground while the airplane turns. In order to compensate for this affect, the tilt of the oscillator must also be taken into account. Certain accelerometers also measure tilt and output the tilt level as a DC voltage, such as the Analog Devices ADXL322.

The mounting requirements for this project need to be adaptable for cases that could include being airborne. This means that the oscillator would not only experience tilt but could also experience vibration in multiple directions.

In order to have an accurate reading of vibration for the feedback loop the speed of the accelerometer is also a critical design constraint. The vibration of the system is a constantly changing parameter. To adequately compensate the feedback for the vibration experienced the accelerometer output would need to happen simultaneously with the vibration change. The overall design has to take into account and minimize the time delay through the system as well.

Using the design constraints discussed above, the Analog Devices accelerometer ADXL322 was chosen. The small, thin, low-power design allows this accelerometer to be an ideal candidate. It has tilt sensitivity and an X and Y channel. Based on the vendor data sheet, the chosen part has a typical vibration sensitivity of 420 mV/g. If any extra

voltage change were to be required, extra amplification could be provided. The product is also very stable over all operating temperatures. This is important because although the crystal is temperature controlled the accelerometer isn't necessarily within that temperature control.

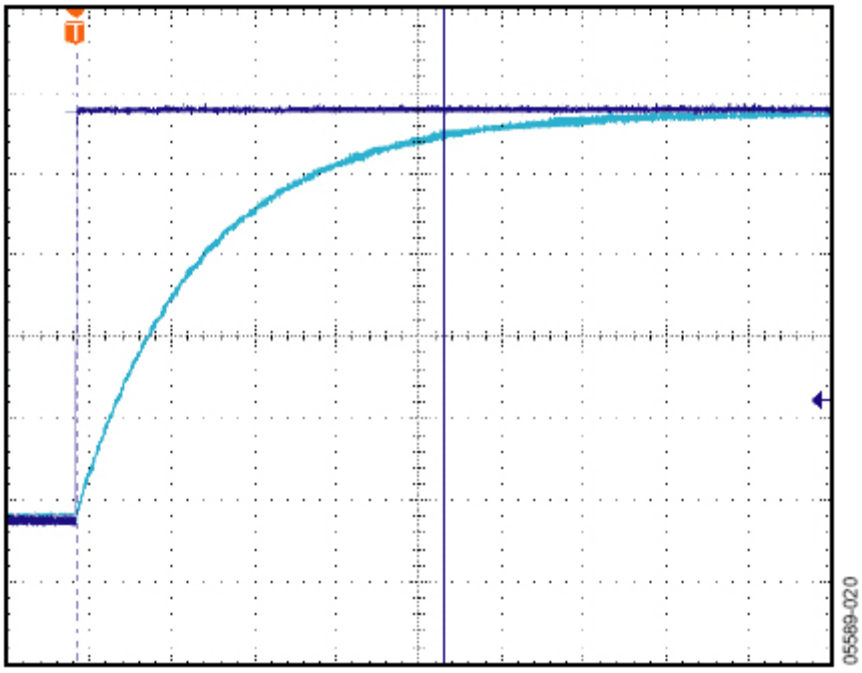

Figure 3-12 Turn on time C_X, C_Y =0.1uF, Timescale 2ms/DIV [19]

Figure 3-12 shows the turn on time of the accelerometer. This data is from the vendor's data sheet and shows the turn on response time of the accelerometer. The turn on time represents the worst case response time for the circuit. A fast response time is necessary to lower the delay of the feedback loop. The vendor supplied data wasn't sufficient for choosing the accelerometer. The responses to different vibration frequencies and vibration levels were measured in order to determine the performance of this accelerometer.

There are three things that the accelerometer needs to measure; the tilt, the acceleration's force and the acceleration's frequency. The affect of changing the tilt and frequency were measured at Rockwell Collins and the acceleration's force change was

given by the vendor data sheet. The first test done of the accelerometer's performance was tilt. While maintaining the same frequency and g level for vibration, the orientation of the accelerometer was changed. The results of this test are shown in Figure 3-13.

Figure 3-13 shows while there is minimal change based on orientation there is a change of the "zero" value of the sine wave. The blue line is the Y axis and the orange line is the X axis measurement. The orientation of the chip for the measurement is shown in the upper left corner of each plot. The orientation change affects the mean value of the output of the accelerometer. This is measured using the oscilloscope and displayed on the output. The X axis and Y axis values see little affect as the orientation is changed; they are both affected equally. It is interesting to note that in the plot where orientation is a side view of the chip, the amplitude of the sine wave falls relative to the level of the others. This is due to the fact that in this orientation the table would be vibrating almost entirely in the Z direction.

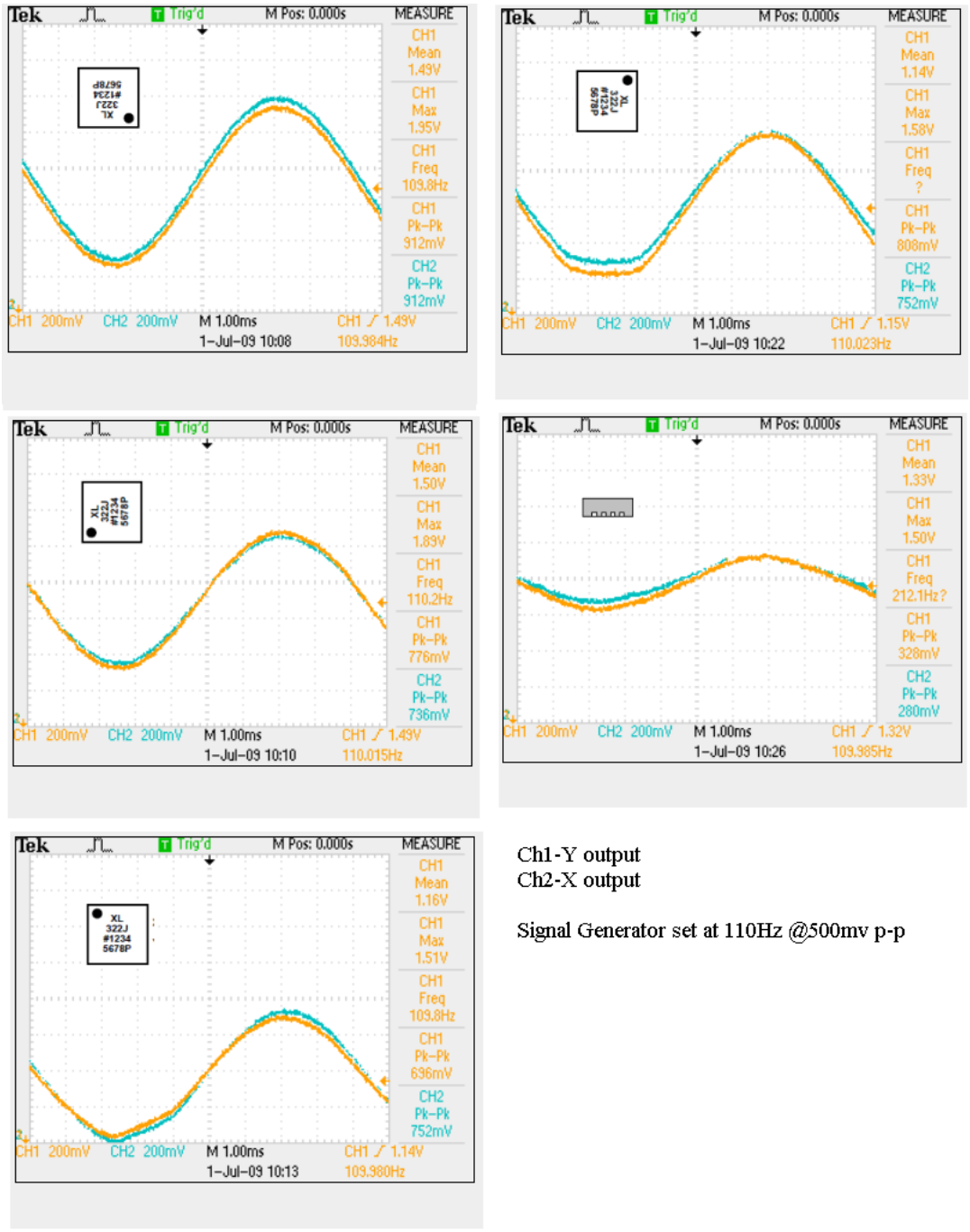

Ch1-Y output
Ch2-X output

Signal Generator set at 110Hz @500mv p-p

Figure 3-13 Tilt sensitivity of accelerometer based on Orientation

With the tilt results in mind the next test was the affect of the frequency vibration on the accelerometer. For this test, the orientation and input voltage were held constant while the vibration frequency changed. Although the vibration voltage input was held constant, the affect on the vibration table itself varied due to the vibration table's internal

limitations; this caused a noticeable change in amplitude based on different frequencies. Because the g level varies based on the voltage input and frequency input, this did not show a fault in the accelerometer's accuracy.

Figure 3-14 shows that as the vibration frequency changes, the output of the accelerometer tracks at the same frequency. The 120 Hz signal shown above has an output frequency of 120 Hz. This allows the frequency of vibration to be accounted for in the feedback control loop.

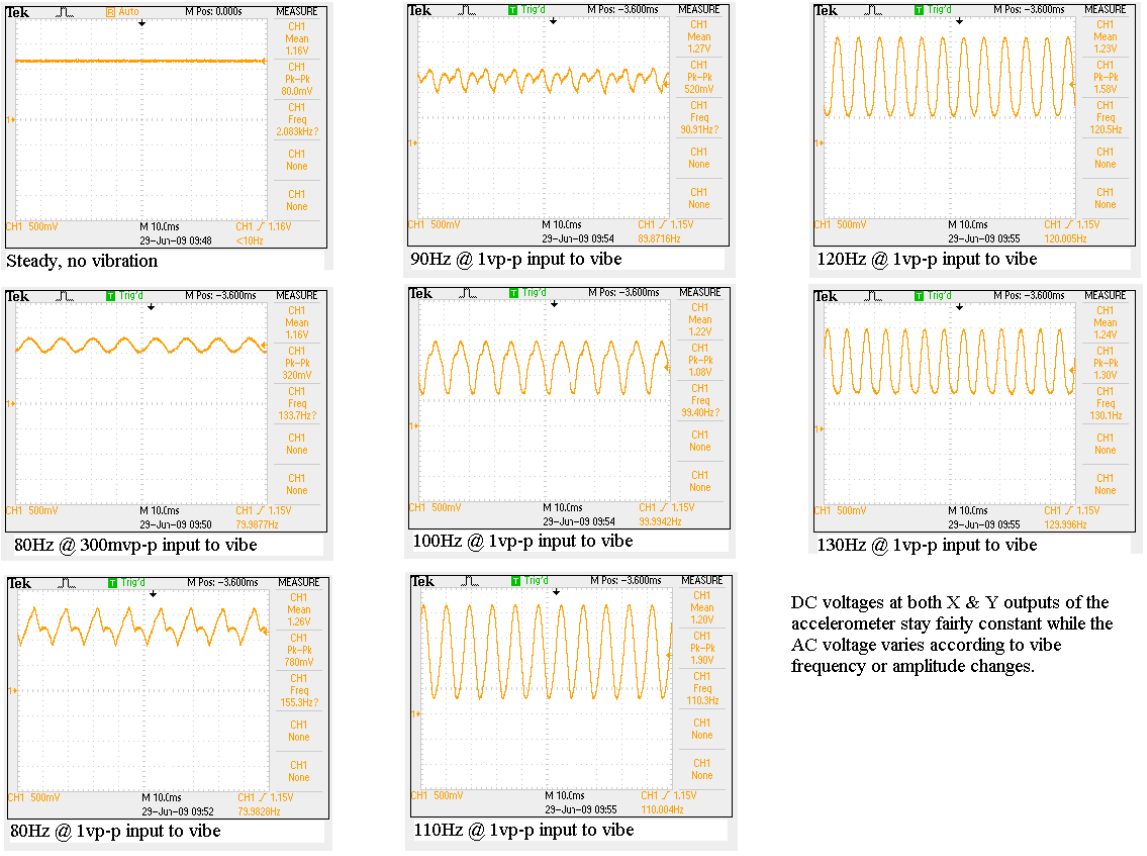

Figure 3-14 Accelerometer Output Based on Frequency Change

The vibration table's input was based on a voltage and frequency from a frequency generator. The limitation of the table is that a signal of 10 Hz and 1 V from the generator would not have the same vibration amplitude as a signal of 100 Hz and 1 V from the generator. This limitation made measuring the accelerometer's vibration

response to varied frequencies but constant amplitude and tilt impossible with an uncharacterized table. Due to this fact those measurements were omitted.

Using this accelerometer a summer circuit could be designed to combine the data from the phase noise integrator and the accelerometer's vibration input.

3.5 Summer Circuit

The summer circuit is designed to combine the output signals from the integrator circuit and the accelerometer. The added channels for the X axis and the Y axis respectively are then used to make up the "I" and "Q" channels to demodulate. The summer circuit concept has varied greatly throughout the design concept based on varied application issues. The design process and changes are outlined in this section.

The summer circuit was originally designed with an accelerometer that would output a DC voltage. Using that assumption an operational amplifier summer was used. This would allow weight to be added to either the level of the vibration or the integrators output. Combining this data together yields a DC Voltage for the X channel and the Y channel. The X channel would be mixed with the 10 MHz output of the oscillator to create the "I" channel. The Y channel would be mixed with the 10 MHz output at 90 degree phase shift to create the "Q" channel.

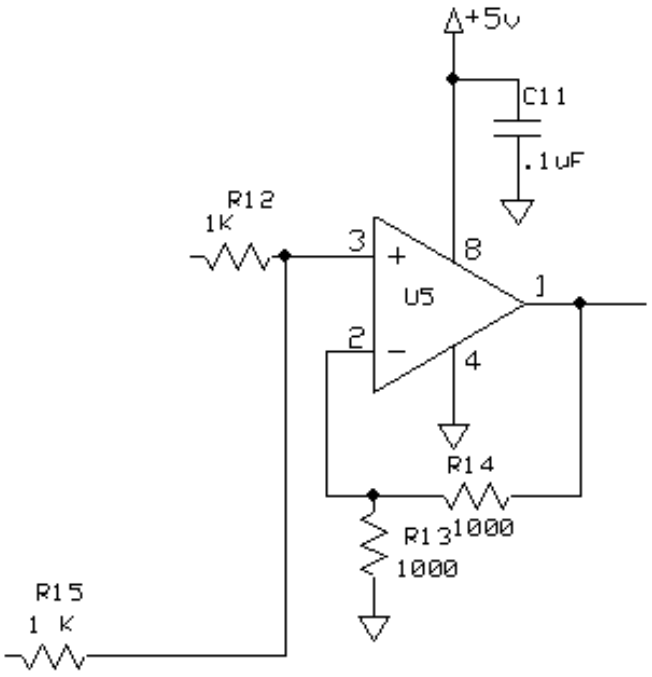

Figure 3-15 Original Summer Circuit Design

Figure 3-15 shows the original design for the summer circuit. R12 and R15 could be changed based on the output range of the integrator and accelerometer respectively. R14 and R13 would be used later on to add gain for the circuit if necessary. The output of this circuit would be a DC voltage based on the different vibrations on each channel combined with the integrator output. This output was then fed into L4 of Figure 3-16 below.

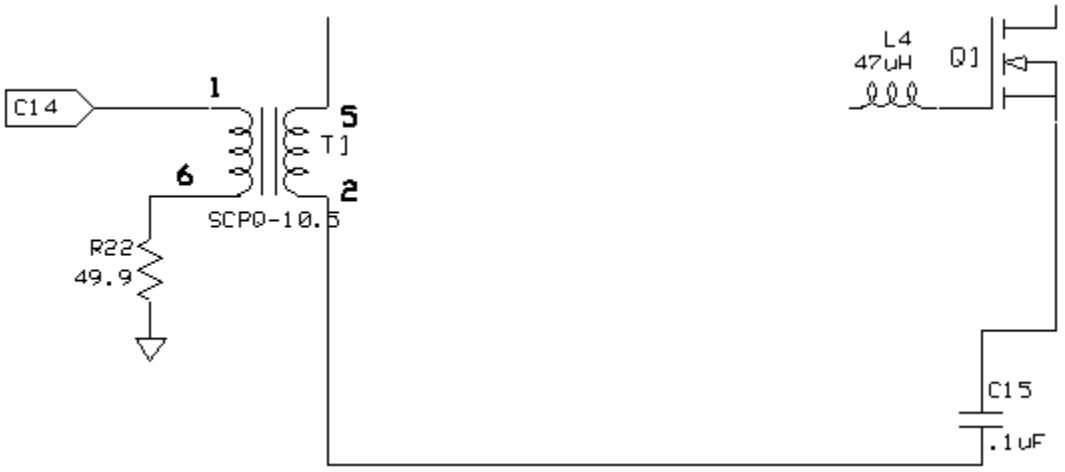

Figure 3-16 Original Mixer Design with Summer Circuit

With the assumption that the output of the summer would be a DC voltage, it could be used so that when there is either a phase noise change or a vibration amount on the circuitry the MOSFET would be in an "on" state. That would allow the 10 MHz output from the oscillator to be passed through the "I" or the "Q" channel. The level of the signal would also depend on the DC voltage input. The 10 MHz signal passes through a 90 degree coupler before being passed to the different MOSFETs. This allows the "I" and "Q" channel to be out of phase. The IQ modulation theory of this summer design is described in the following section.

It was determined that a lumped component's version of the 90 degree coupler would be most ideal due to size concerns at 10 MHz. The design shown in Figure 3-17 was chosen for the initial design.

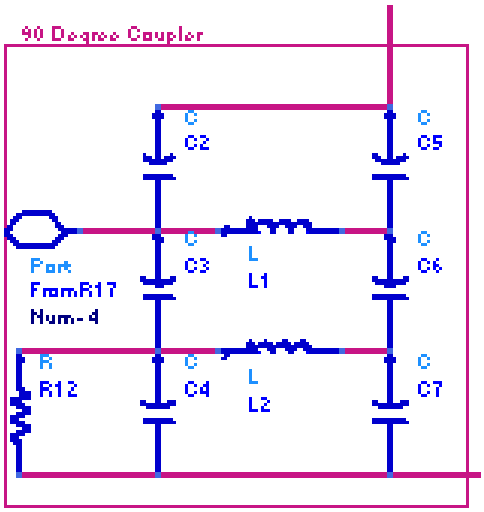

Figure 3-17 90 Degree Coupler Design

This coupler design took 10 MHz in from the Port shown above and had the other input at 50 ohm to ground. The L's and C's were chosen based on the following equations.

$$K = |S_{2,1}|$$
$$M = KL$$
$$C_1 = \frac{L - M}{2Z_0^2}$$
$$C_2 = \frac{MC_1}{L - M} = \frac{KC_1}{1 - K}$$
$$f_0 = \frac{1}{4n\sqrt{2(L + M)C_1}}$$

For these equations, Z_0 was 50 Ohm. C_1 is the same as C2, C5, C4 and C7 on the schematic and C_2 is C3 and C6 on the schematic. L is both L1 and L2 on the schematic. Based on those equations the simulation results of the circuit were obtained and are shown below.

Figure 3-18 shows that the phase difference between S(1,1) and S(1,2) is 90 degrees apart at 10 MHz while their insertion loss at 10 MHz is within 1 dB. This 90

degree coupler would allow the adequate phase change between the "I" and "Q" channels as needed.

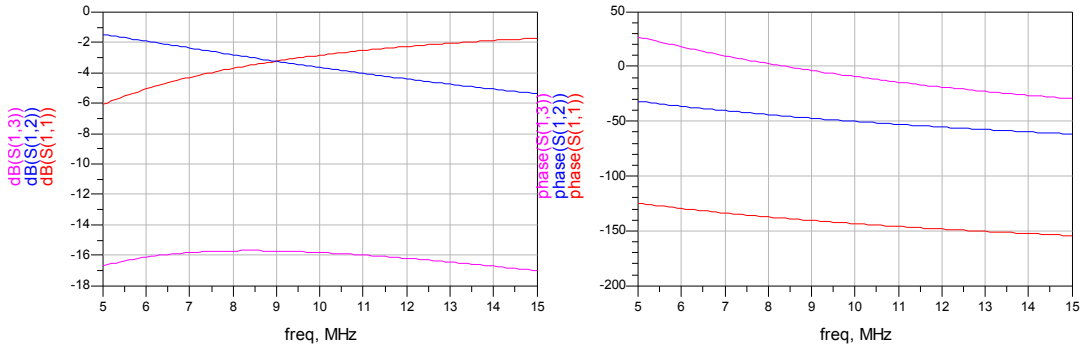

Figure 3-18 Simulation Results 90 Degree Coupler

To further reduce board allocation space for the coupler, an off the shelf 90 degree coupler was used. This was the first design change that occurred during the design process of the summer circuit. This would cut down on trouble shooting, reduce the tuning time, and improve performance. The data sheet's results are shown in Figure 3-19 below. This shows that this particular coupler is matched at 10 MHz and the outputs have an identical insertion loss of 3 dB. The simulation of the other circuit yielded a design more closely matched to 9 MHz with the kit components available in the lab.

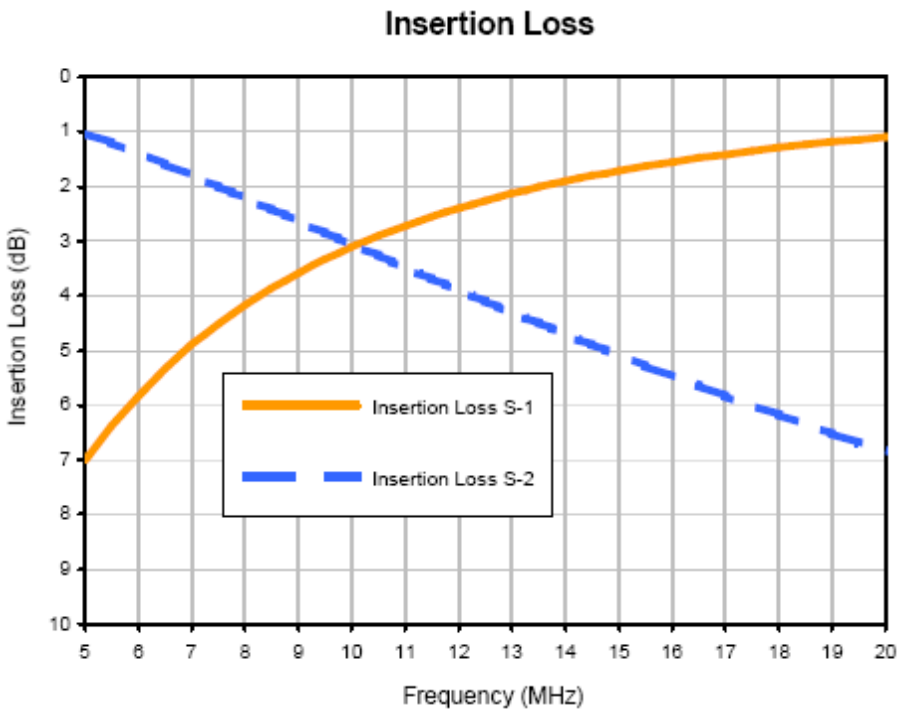

Figure 3-19 Insertion Loss of 10 MHz 90 Degree Coupler

The design was changed again with the chosen accelerometer's tilt and frequency tracking capabilities in mind. With the accelerometer having the capability of measuring vibration frequency and tilt, it was no longer necessary to combine it at the summer input. Instead the phase noise integrator circuitry change could turn on each channel directly; this would allow each channel to be on when experiencing a change in phase noise.

Two benefits of this design are that this will account for changes in phase noise without vibration and eliminate feedback when the phase noise doesn't change under minimal vibration. When there is a phase noise change, but there isn't any vibration change on the system, there is still a feedback input to correct the phase noise change witnessed based on the MOSFET input. Conversely if there is vibration which doesn't affect phase noise there is no need to feedback any change to the oscillator.

The 10 MHz signal wouldn't be needed using the MOSFET design. Instead the accelerometer output could be passed through by the MOSFET. With the accelerometer

having the vibration level, frequency and tilt accounted for in the amplitude and offset of the output this would all pass through when there was a phase noise change.

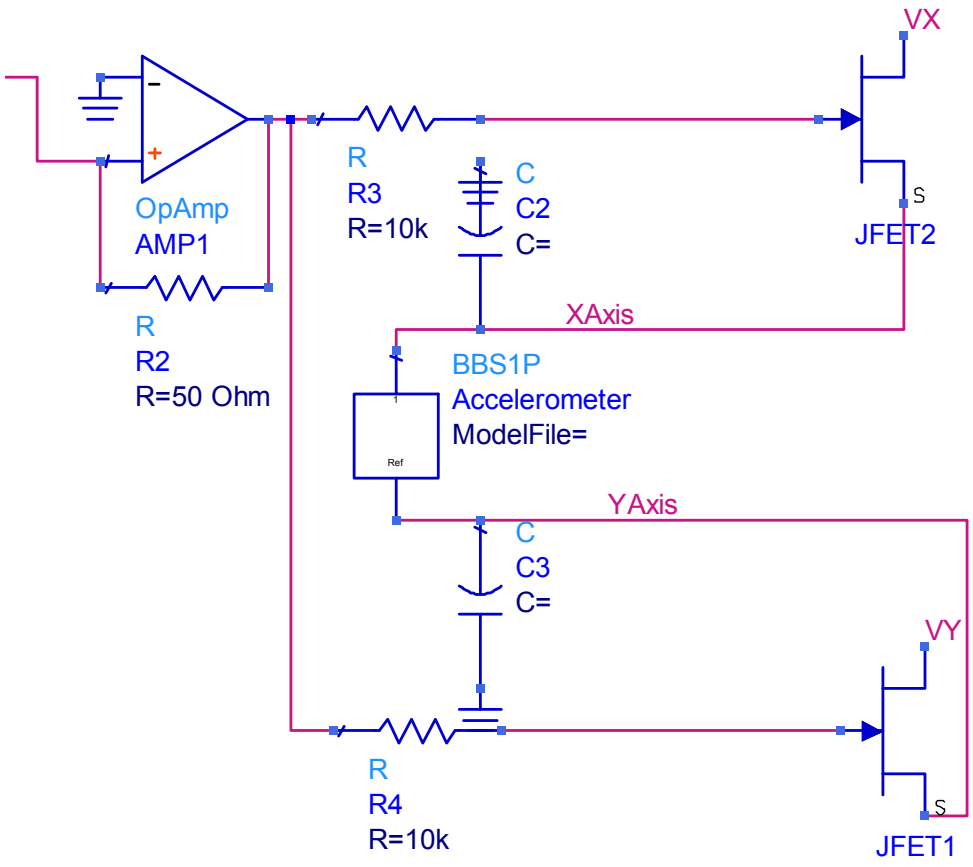

Figure 3-20 Summer Circuit Design

Along with the changes outlined above, the Operational Amplifier was changed to positive feedback. The outputs V_X and V_Y are then the scaled output of the Accelerometer based on the phase noise integrator's output. The X and Y axis make up the "I" and "Q" channels of the modulator.

The FET mixer's gain can be calculated as [20]:

$$G_c = \frac{G_{m,\max}^2 R_L}{16\omega_{RF}^2 C_{gs}^2 (R_S + R_i + R_g)} \quad \text{[Equation IV-11]}$$

Where the R_L is 50 ohm and C_{gs}, R_S, R_i and R_g are all given by the FET characteristics.

Based on actual results of the accelerometer and the results of the phase noise integrator circuit, a simulation was completed. The simulation looked at the affect of the change in the phase noise integrator voltage, the affect of the changes in the tilt and the changes of vibration amplitude and frequency. The Figure 3-21 shows the schematic used. For this simulation a realistic MOSFET model was used with the characteristics supplied by the vendor. The vendor part is International Rectifier IRF7303.

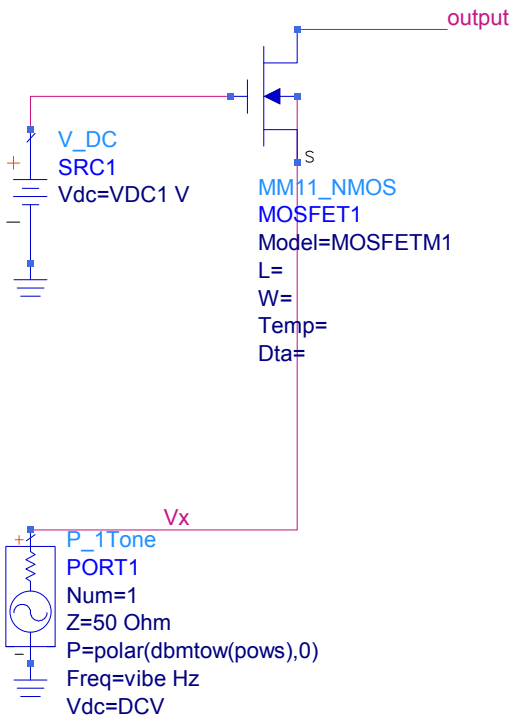

Figure 3-21 Summer Circuit Simulation Schematic

Using the above schematic the results at point output were observed under a variety of conditions. The phase noise integrator voltage was changed from 0 VDC to 2 VDC to see what happens as the MOSFET is turned on. The amplitude of the signal from the accelerometer was increased to simulate a change in vibration force. The offset

voltage of the accelerometer signal was increased to simulate a change in tilt of the OCXO. The first conditioned observed was the turn on test.

The signal in red is the output of the circuit, while the blue signal is the output of the accelerometer. Figure 3-22 shows that as the voltage is increased the output does increase correspondingly. This would give higher weight to an increased change in phase noise. This also shows that when there is no phase noise integrator output, the output would be low and a constant DC output.

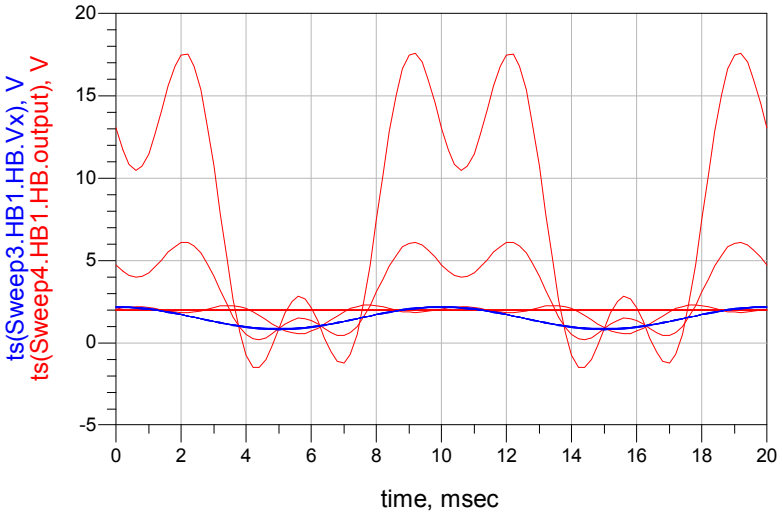

Figure 3-22 Summer Circuit Output with Phase Noise Integrator Varied

The next simulation varied the offset voltage to see the effect of tilt on the output of the summer circuit. This is shown in Figure 3-23 below. Based on the results it can be noted that as the tilt level increases the output level increases with it. This means that the affect of the tilt on the crystal would be taken into account with how severe the DC voltage is, just as expected.

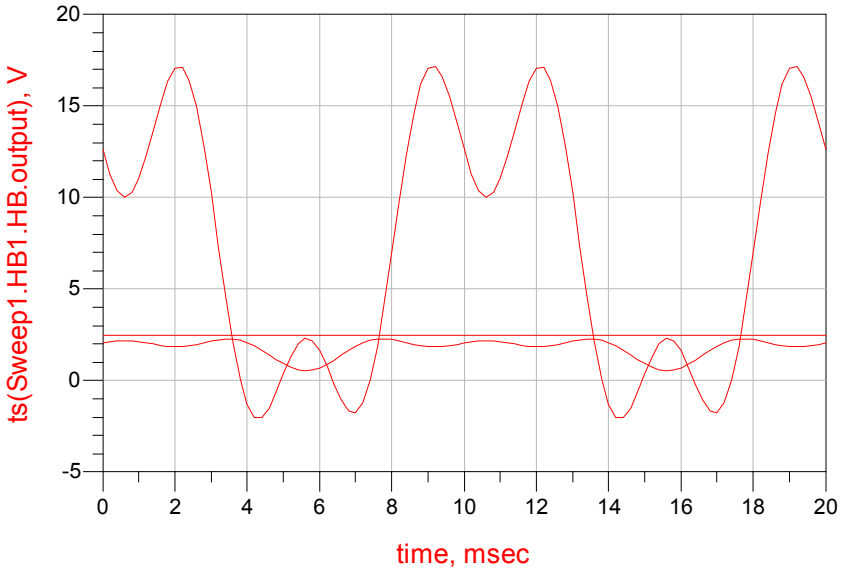

Figure 3-23 Summer Circuit Simulation Results Varied Tilt

The final simulation involved changing the force of the acceleration by varying the amplitude of the signal input. As the amplitude of the input is increased, the amplitude of the output also increases in Figure 3-24. This means that as the vibration level increases the output voltage would also increase accounting for that added vibration and feeding back a higher voltage. With all these results in mind the next stage is the IQ modulation circuit.

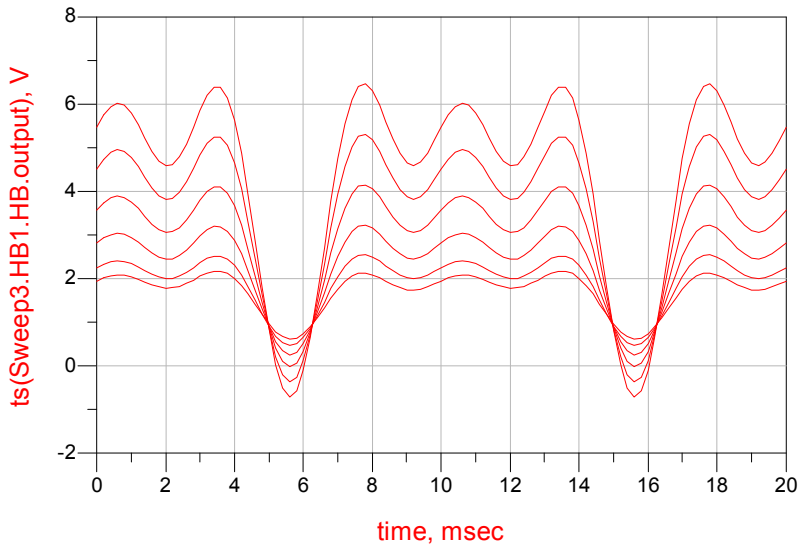

Figure 3-24 Summer Circuit Simulation Results Varied Acceleration Force

3.6 IQ Modulation Circuit

The IQ modulation circuit design involves the recombination of the X axis and Y axis data to form a single DC output for feedback. The output of this circuit would be the input to the feedback portion of the design.

While the circuit is called the IQ modulation circuit, it is actually a demodulation section. The name of IQ modulation circuit comes from the conceptual idea that the feedback is similar to that of IQ modulation. The similarity is that the "I" and "Q" lines have different sets of data on them. In this case, the "I" has the X axis vibration data and the "Q" has the Y axis vibration data. This data is then mixed with the RF frequency at a 90 degree phase shift and combined to have a transmittable signal at the RF frequency that includes both "I" and "Q" data on one channel.

The X and Y channels of this system contain the frequency of vibration inherent from the accelerometer. The vibration frequency was used as the LO frequency for the

IQ modulation scheme. This allowed the drop of the 10 MHz LO input to the Summer Circuit. The X and Y channels are then combined together to create one channel of DC voltage output to feedback into the crystal oscillator.

The circuit itself has two main stages: the first stage is a low pass filter and the second is a mixer circuit to recombine the data. The low pass filter is designed to remove all frequency results over the highest level of vibration concerned, in this case anything over 2.5 kHz would be acceptable. The main goal of this low pass is to avoid taking away any frequency data while cutting off any residual 10 MHz signal.

Due to this fact, the cutoff frequency was chosen to be 4 MHz, in order to allow maximum gain flatness between 10 Hz and 2 kHz and a significant loss at 10 MHz. The following equations were used to determine the desired values for the inductors and capacitors.

$$C = \frac{c_n}{(2\pi f_c)R_L}$$

$$L = \frac{l_n R_L}{(2\pi f_c)}$$

$$c_n = 2$$

$$l_n = 1$$

$$C = 1592\,pF$$

$$L = 199nH$$

For design concerns, off the shelf components of similar size were chosen. These were 1420 pF and 200 nH. Figure 3-25 below shows the design based on the common components. For this simulation, ideal components were used without taking into account the parasitic effects that would occur.

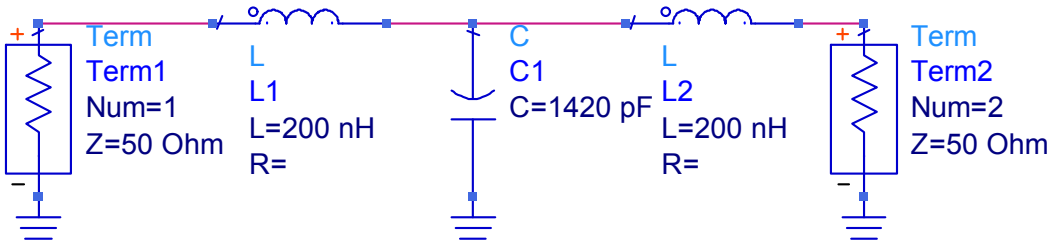

Figure 3-25 Circuit Diagram Low Pass Filter IQ Modulation

Simulating the common components design led to the close in results in Figure 3-26. The filter performance shows that there is a 7 dB loss at 10 MHz, knocking down any high frequency signal that comes through. Close in frequencies of the pass-band have a very low and consistent loss. It is important to determine the significance of the part change to the overall circuit, however, so another simulation was done with these results compared to the ideal component results.

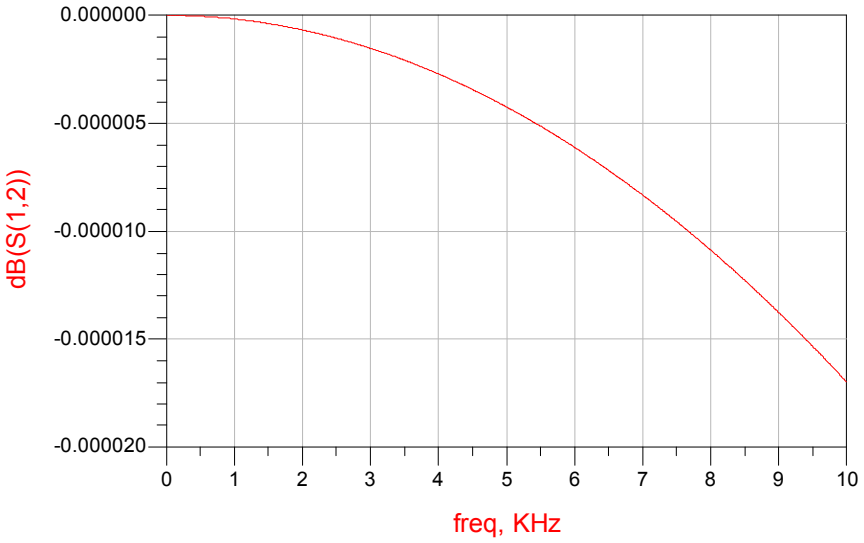

Figure 3-26 Close In Filter Performance

The ideal components are in blue while the realistic commercial off the shelf available components were in red. This shows that while the rejection of the 10 MHz

signal with the ideal components would be greater, the delta between the two filters isn't great enough to redesign.

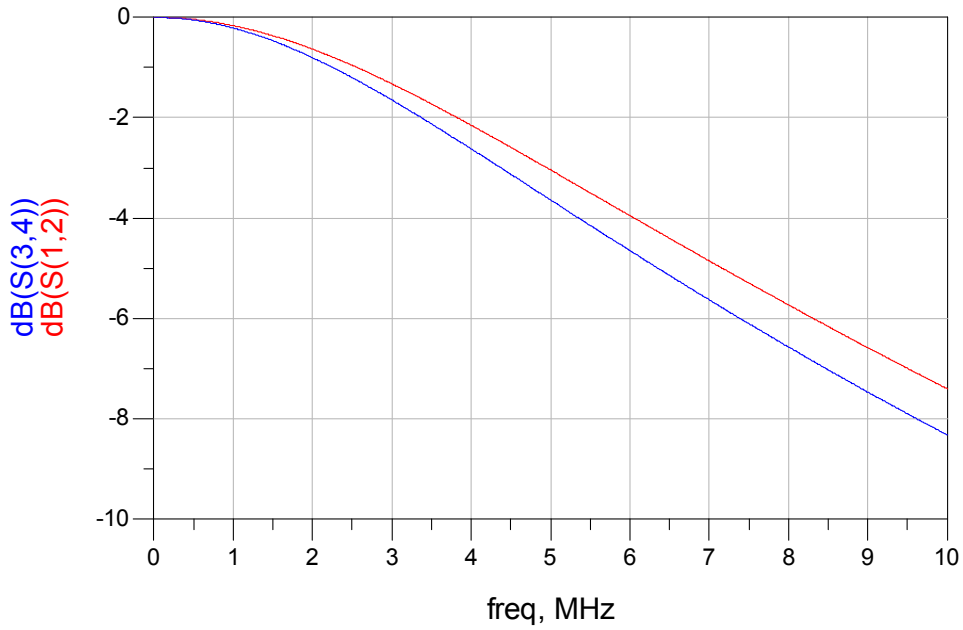

Figure 3-27 Ideal vs. Realistic Component Results

The second part of the IQ modulation portion of the circuit design is the recombination of the two signals. This is done with a mixer. The mixer multiplies the two frequencies together to create one signal of DC voltage with the information from both signals. For the mixer, an ideal mixer was used for simulations. The mixer was chosen to be an off the shelf component for the design.

The design for the summer, the low pass filter and the mixer were all combined to one simulation result. For this simulation, actual results were used from test for the inputs from the accelerometer. Based on the results of the accelerometer tests there were multiple simulations that took place. This would allow the observation of the affect of

both tilt and vibration on the IQ modulation results. The schematic used for the tests is shown in Figure 3-28.

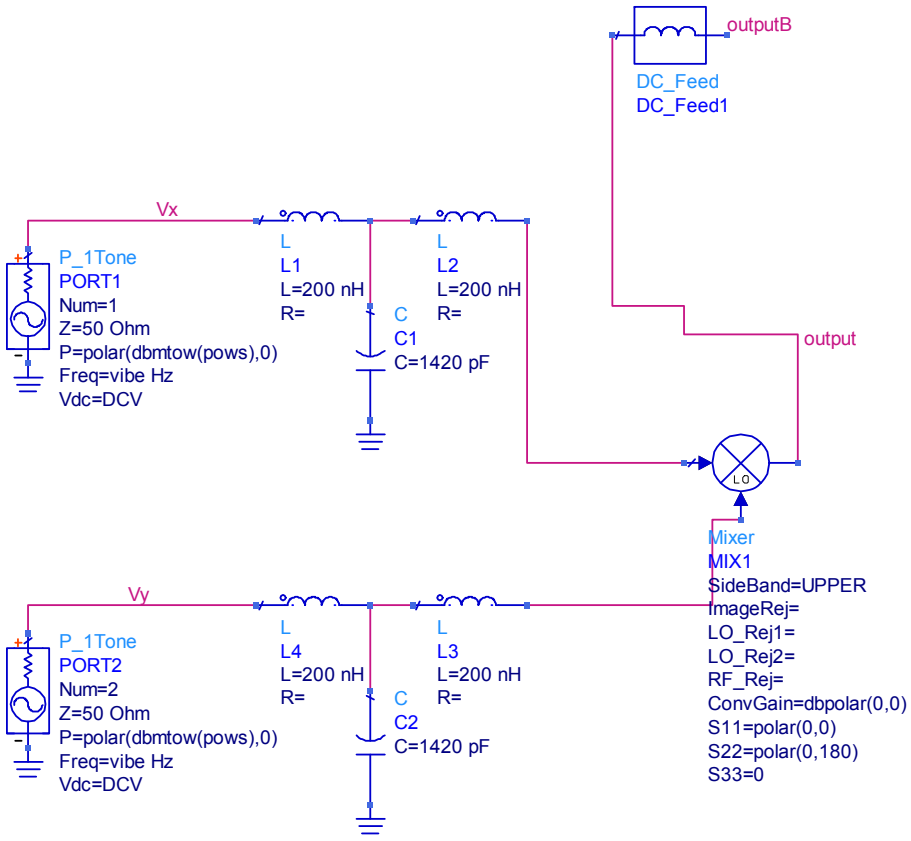

Figure 3-28 IQ Modulation Simulation Results

There is a DC_Feed block added for the simulation. This would be changed to a low pass filter for the final feedback circuit with a steep roll off. The ideal component was used for ease of simulation in this section.

All tests assumed the summer circuit would be on the whole time. The first test holds the vibration steady while changing the tilt. For the simulation, tilt was changed between 1 to 2 VDC to simulate the full possible range of output of the accelerometer. The blue signal shows the results prior to the DC_Feed block and the red line shows it after the DC_Feed block. The simulation shows that after the mixer the feed back

voltage would be affected by the tilt from 0.6 Volts to 1.4 Volts approximately. This shows that the IQ modulation circuit is doing what it should to account for tilt in the system.

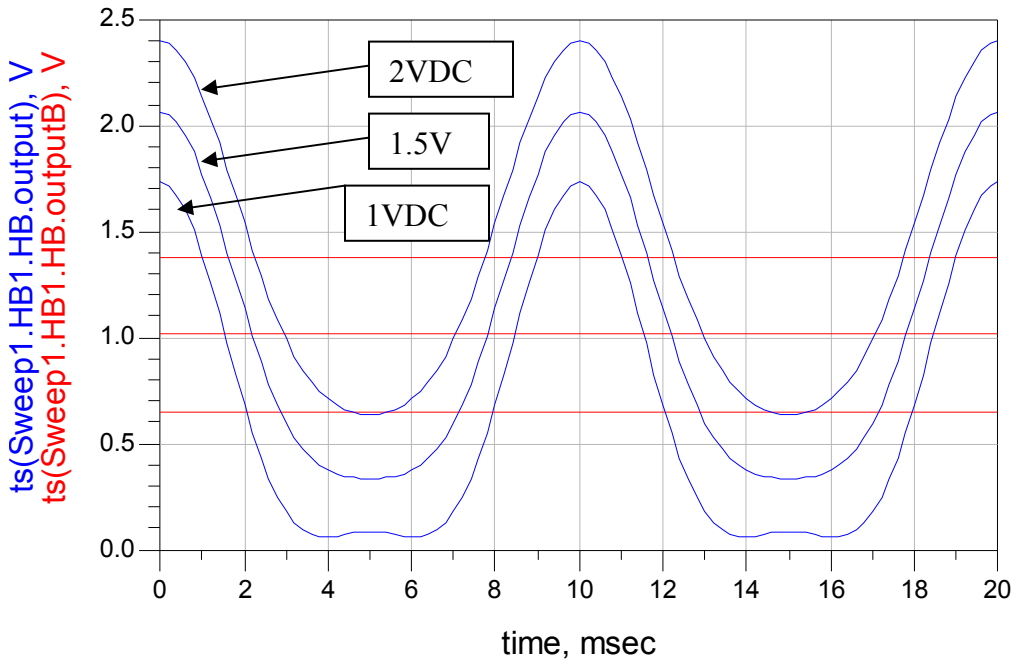

Figure 3-29 Simulation Results of Tilt affect on IQ Modulation Circuit

The next test preformed was holding the tilt steady while changing the amplitude of the accelerometers output signal. This would correspond to an increase in the force of acceleration on the crystal oscillator. Figure 3-30 shows the results of the simulation with varied output amplitudes and constant tilt. A conservative approach was taken with the simulation to try and show realistic amplitude changes throughout a period of performance. With minimal change there was still a measurable voltage change.

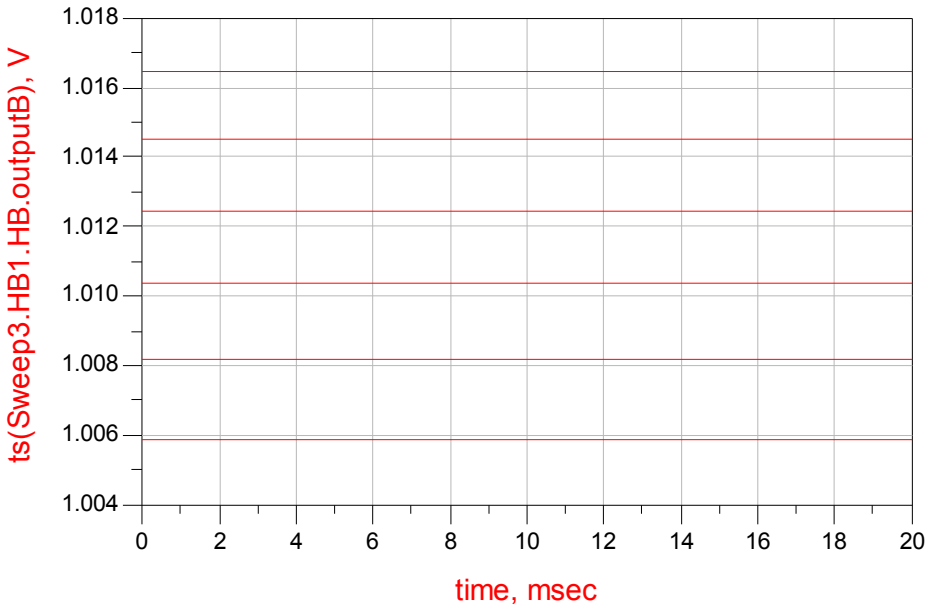

Figure 3-30 IQ Modulator Circuit Simulation Based on Acceleration Force Change

Based on the results of both Figure 3-29 and Figure 3-30, it is shown that with the simple mixer design for IQ modulation, a voltage change can be obtained based on both acceleration force and tilt if the accelerometer is fed directly into the system. The next step was to determine the results with the simulation of the summer circuit and compare the results. For this simulation the same MOSFET model was used, the International Rectifier IRF7303. A realistic Mixer was used as well, but the passive components were all ideal without taking into account the parasitic effects.

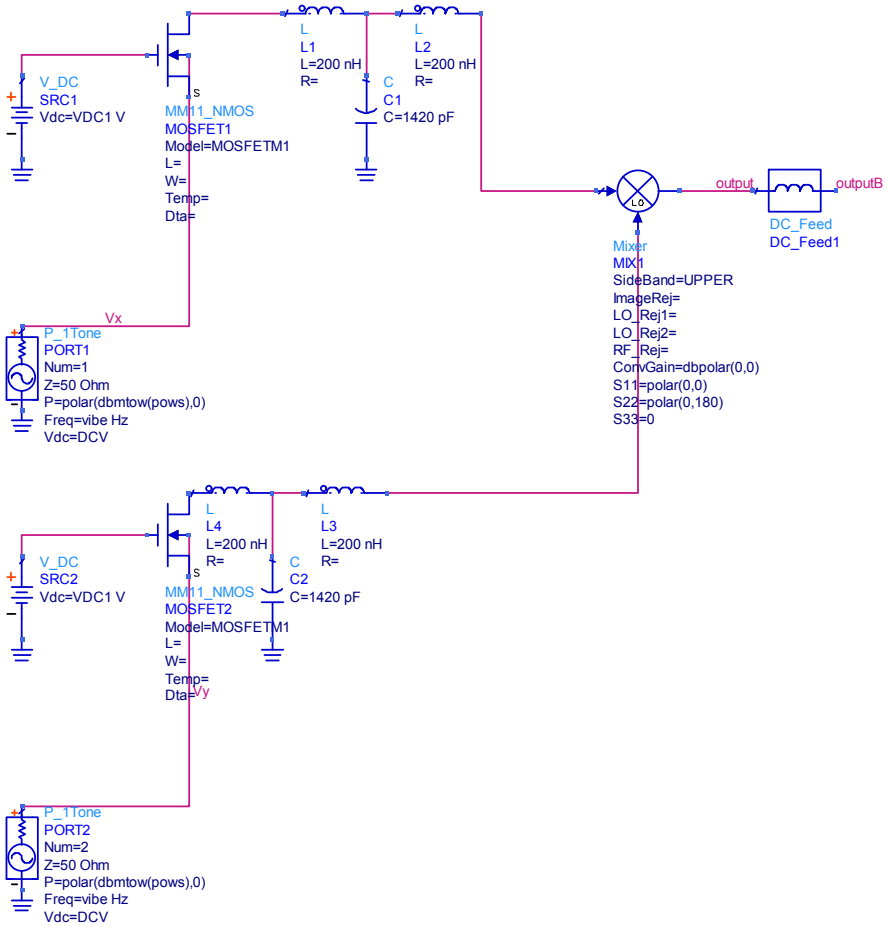

Figure 3-31 IQ Modulation Chain Simulation Schematic

Figure 3-31 shows the full IQ modulation chain. This takes into account everything from the oscillator output with measured results for vibration for the accelerometer. It also assumes that the phase noise integrator output, the force of acceleration and the tilt are all variables. The initial simulation was to verify the system reacts properly as the phase noise integrator output is varied from 0 to 2 Volts. This range would allow the MOSFET to perform while passing the accelerometer data, limiting the accelerometer data and stopping the accelerometer data completely.

The output of the phase noise integrator is shown in Figure 3-32 to have an affect. As the output increases, there is an increased voltage response after the DC_FEED block.

This shows the ability of the IQ modulation circuit to compensate for a change in phase noise performance without a change in vibration level being involved.

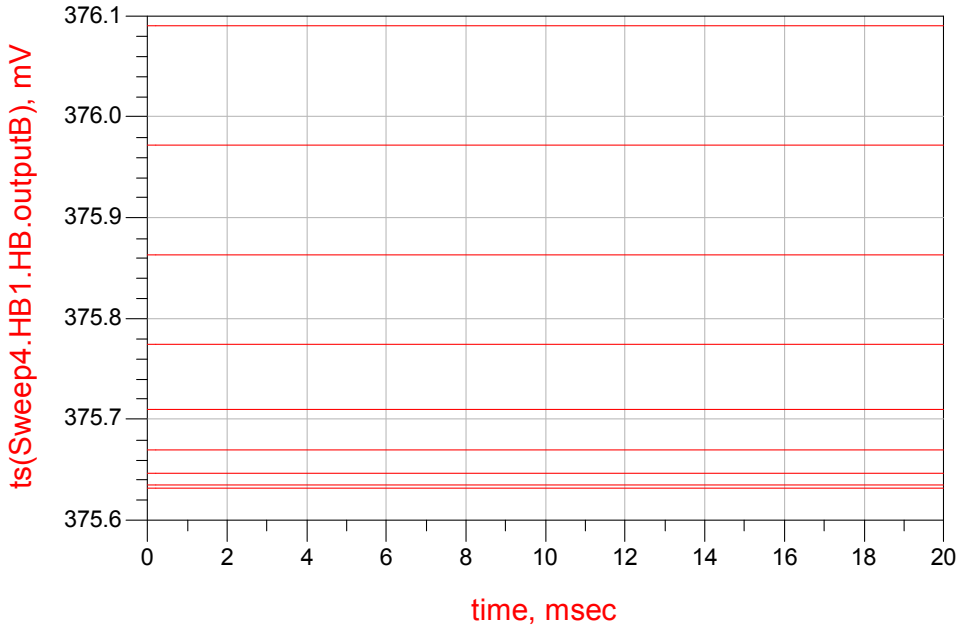

Figure 3-32 IQ Modulation Chain Variable Phase Noise Integrator Output

The amplitude of the accelerometer output was varied to show the change that could happen with different acceleration forces. Like that of the phase noise integrator, the change in acceleration force increases the voltage output of the system. Using this, it is possible to design the feedback to allow the voltage to change from 0-5V to maximize the change in frequency and the minimization of phase noise.

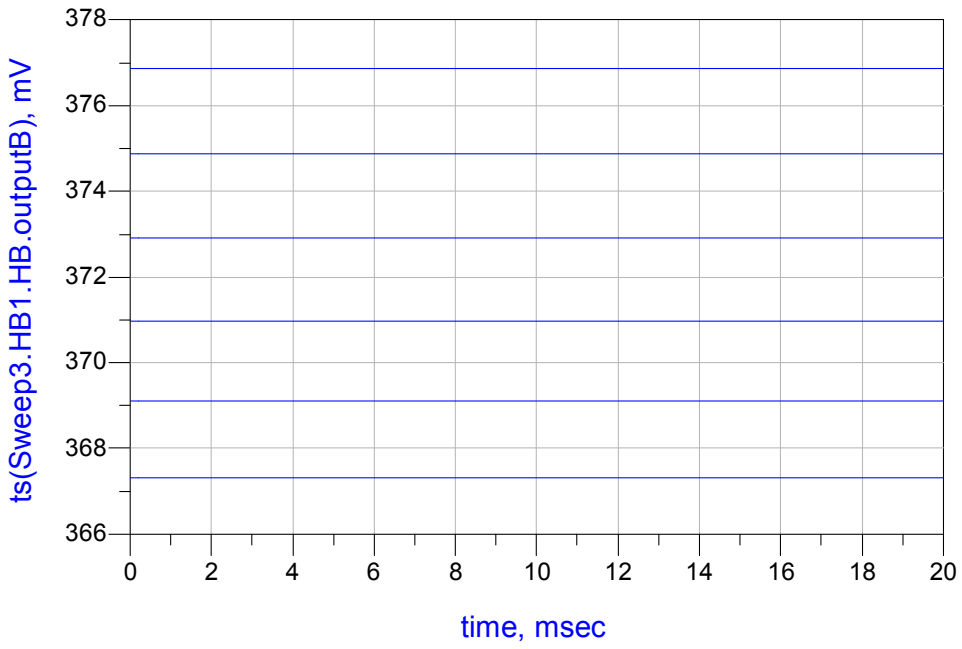

Figure 3-33 IQ Modulation Chain Simulation with Variable Acceleration Force

The last remaining simulation involves the change of the tilt on the system. The red signal is the output before the DC feed block, while the blue output shows the level after the DC feed block. Along the same lines as Figure 3-33 and Figure 3-32, Figure 3-34 shows the change in the DC voltage of the output. Again this voltage isn't at the 0 to 5 volt range, but all show a similar change in voltage based on their respective level change. Based on this, a circuit could be developed to increase that voltage with a realistic DC block.

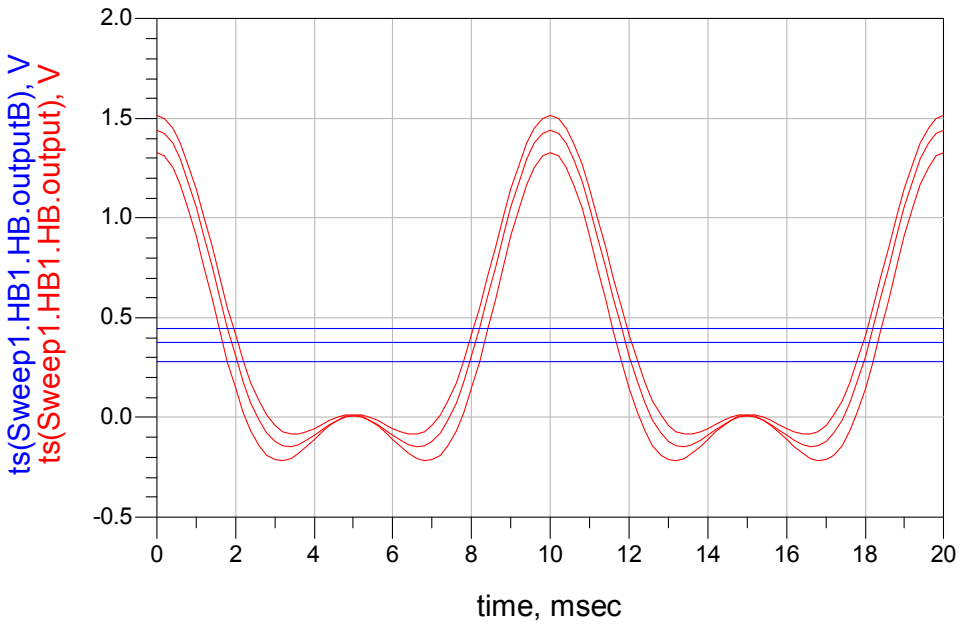

Figure 3-34 IQ Modulation Chain Simulation with Tilt Variable

3.7 Feedback Circuit

With the voltage change being established for the IQ modulation, a block needs to be added to relate that change in voltage to the oscillator. The block to do this is the Feedback Circuit block. The feedback circuit block is made up of two parts. The first is the DC Feed design and the second is the circuit to take the voltage change and relate it to the oscillator. The DC Feed circuit ideally would be an inductor with infinite inductance. This is not realistic, however, so a low pass filter with a very steep drop could be implemented.

The frequencies of vibration are low, however, so the f_C, cutoff frequency, would have to be less than 10 Hz where the vibration specification would begin. This filter can't be designed using normal filter calculations methods with parts that are available. The largest size inductor available for this project was 10 mH. Based on that and the

largest capacitor available, 470 µF, a 5 pole filter was devised and optimized to fall within certain parameters.

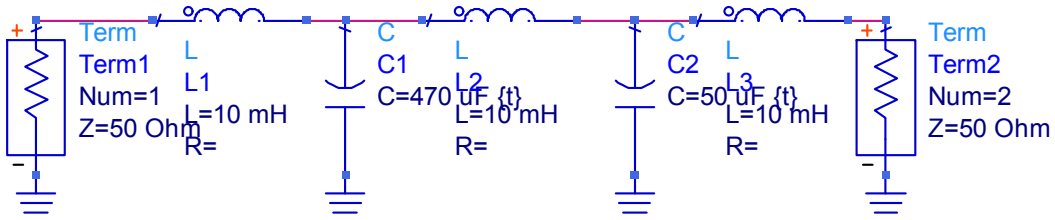

Figure 3-35 DC Feed Filter

Using the largest Inductors available and making an LC style filter, the capacitors were varied with different values available in the lab to come up with an optimal design. Using this design route, it was determined that using the largest value capacitor in C1 would affect the slope of the drop-off the most. However as C2 varied there was a peak that arose in the filter. In order to keep the notch under 10 dB, C2 had to be lowered to 50 µF. This kept the slope at a steep decline while compensating for the peak enough to assure the filter would be an adequate DC feed circuit.

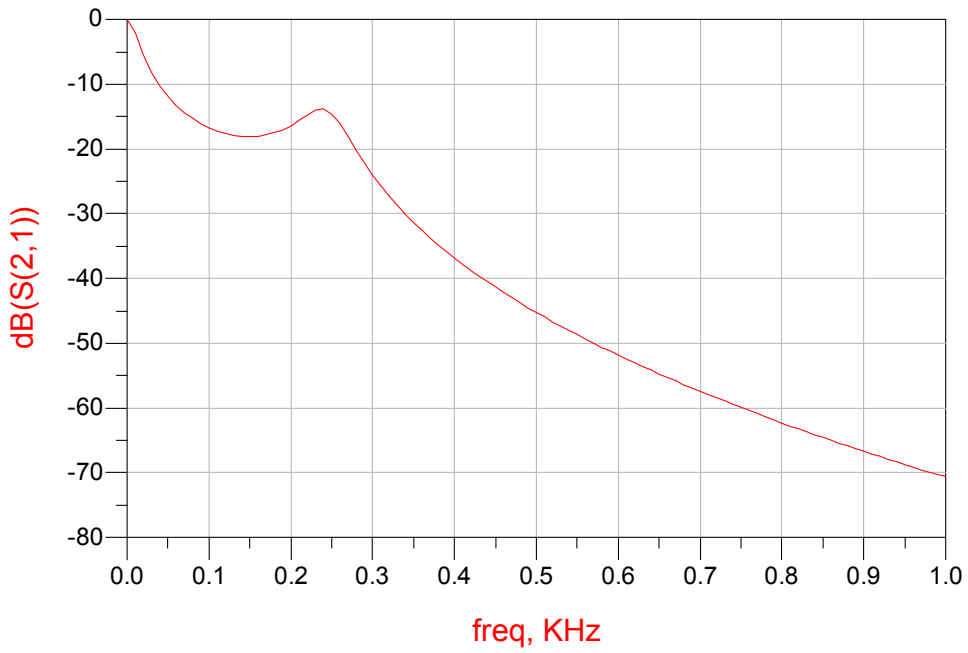

Figure 3-36 DC Feed Circuit Simulation Results

From Figure 3-32, Figure 3-33, and Figure 3-34 it can be seen that the changes are generally within 0.2 and 0.5 VDC. In order to maximize the change in the oscillator, it needs to be the full range of the input. This means that it needs to go to 5 VDC. In order to accomplish this, an op amp circuit was used with gain of 10 to change the range from 2V to 5VDC.

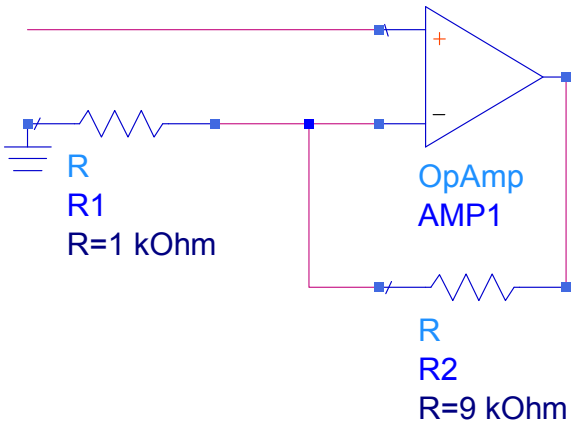

Figure 3-37 Gain Feedback Circuitry

The Figure 3-37 shows the gain circuitry for 10 times the voltage. The gain was determined as follows:

$$G = 1 + \frac{R_2}{R_1}$$

$$G = 1 + \frac{9k}{1k} \qquad \text{[Equation IV-11]}$$

$$G = 10$$

A major concern of the Gain Feedback Circuitry is the stability of the system. As the circuit rotates the forces on it change. This is taken into account with the tilt sensor, however if the crystal is flipped 180 degrees the tilt output would remain unchanged while the force would change the crystal output from positive to negative change in frequency due to the added force. If the correction gain circuit only decreases the frequency the delta frequency would get worse until the gain is driving the rail voltage and the oscillator is at the lowest possible frequency. For this circuit it was assumed the crystal would never be flipped 180 degrees assuring that the tilt sensor was adaquete to assure the correct voltage applied and stability is reached. Adding a second accelerometer in a different orientation could also be done to get the correct vector of force, this would allow full rotation of the crystal in space.

Combining all the circuits together would give the feedback voltage level given at certain vibration levels. This was simulated with a change in tilt, vibration and phase noise integrator input voltage, as has been done in all previous simulations.

3.8 Overall Circuit

The overall circuit design was split up into several blocks. These blocks were discussed in the section above and their individual results and successes were discussed in detail. The remaining effort was to reconnect the blocks into an overall schematic for a complete phase noise reduction IQ circuit.

Based on the block diagram shown in Figure 3-1, a schematic was devised for the whole system. This took into account the block results individually and compensated for those appropriately.

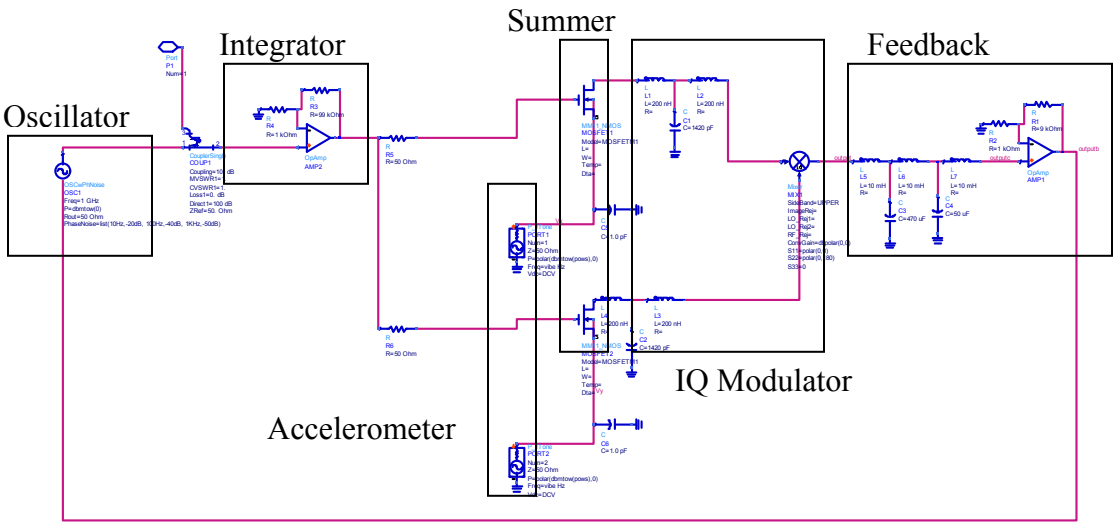

Figure 3-38 Complete Circuit Schematic

Shown in Figure 3-38 is the schematic diagram for the full system. This shows the feedback line going from the feedback circuitry then back to the oscillator's output. It

then goes through a coupler back to the feedback IQ loop to continually change the phase noise as vibration continues to change and occur.

The first simulation of the overall feedback loop takes place over the phase noise integrator changing. The following was obtained with the full circuit. The blue line is the output before the amplifier feedback circuit. As expected, when the phase noise experiences a change in voltage there is a near 5 VDC level of feedback. This corresponds to the level of vibration at the time that the summer circuit is on.

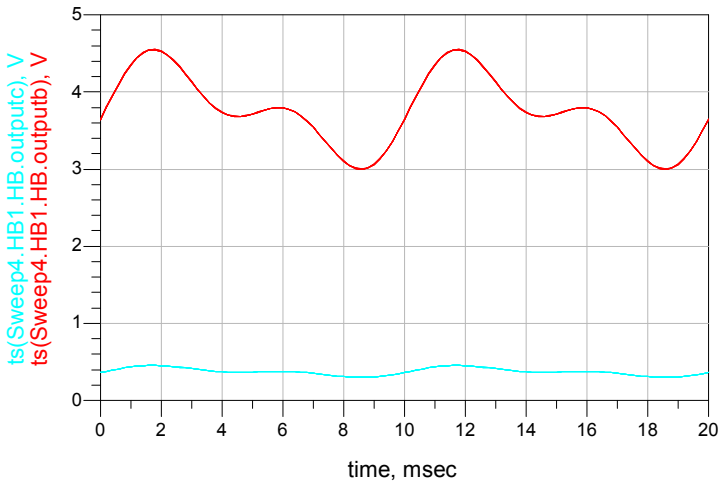

Figure 3-39 Feedback Voltage with Phase Noise Integrator Input Variable

Next the acceleration force level was changed with a constant tilt and phase noise integrator input. Figure 3-40 shows the affect of varying the amplitude of the signal input to the vibration table. Based on these simulation results, the change based on vibration level can be seen and the feedback would change the frequency accordingly.

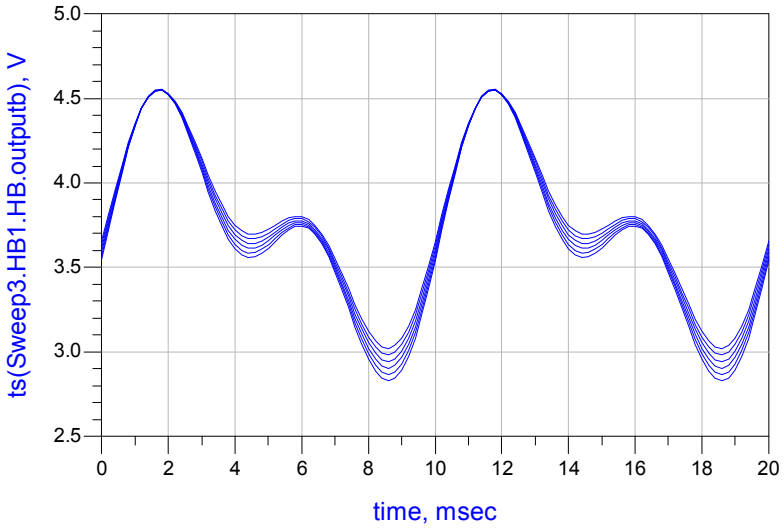

Figure 3-40 Feedback Voltage Level with Acceleration Force Variable

The tilt results have the largest effect on the change of the frequency. This is based on the simulation of changing the tilt while keeping the acceleration force and phase noise integrator constant.

The blue line represents the voltage that is fed-back to the oscillator. This voltage is shown to be on average 3V to 5V based on the level of tilt shown in the circuitry. This change will affect the phase noise and feedback accordingly to change the frequency and lower the phase noise. Overall, the IQ modulation system is shown to generate a variable voltage input to the oscillator based on vibration level, tilt and phase noise integrator level.

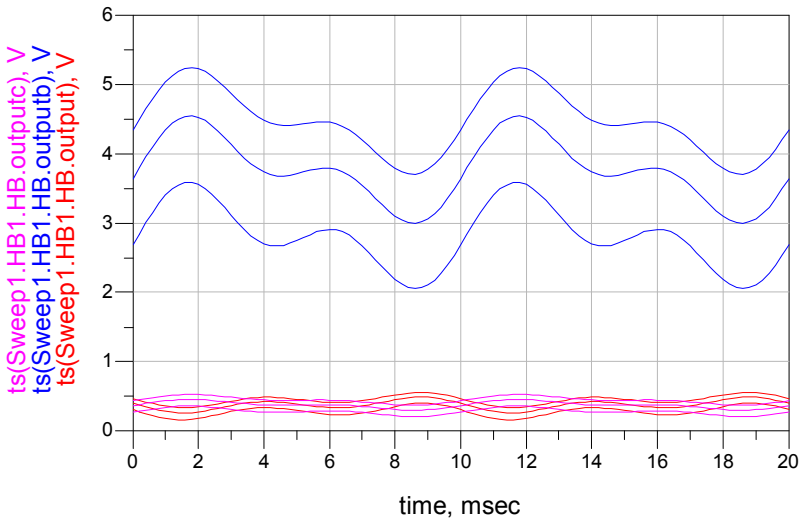

Figure 3-41 Feedback Voltage Level with Tilt Variable

The overall circuit feedback loop is shown to provide a ranged voltage based on the variables known to affect the phase noise change, as well as a measurement of the phase noise integral itself. The feedback itself affects the oscillator ±0.55 ppm from 10 MHz. Vibration affects the phase noise as follows. This equation represents the single side band phase noise under random vibration. For this equation Γ*in* is the G sensitivity of the crystal, GLevel is the acceleration force of vibration, *fc* is the carrier frequency, and *Foff* is the offset frequency due to vibration.

$$RandVib = 20\log(\Gamma in \cdot \sqrt{2 \cdot GLevel} \cdot \frac{fc}{2Foff}) \quad \text{[Equation IV-12]}$$

The way the other vibration reduction schemes reduced this is by reducing GLevel. By reducing the difference between *fc* and *Foff* which is done by up to 0.55 ppm with the IQ modulation scheme shown above, the overall phase noise is also reduced by that same factor.

Based upon this theory the IQ modulation phase noise reduction technique is shown to be viable with the feedback results shown in previous sections.

3.9 Innovation

Using the IQ modulation phase noise reduction technique shows the ability to improve the phase noise of the system during vibration. It also has a clear advantage over the mechanical vibration isolator design in both size and weight of the system. Polarization-effect tuning circuits have shown historic phase noise reduction in practice, but have limitations.

IQ modulation technique takes advantage of closed loop feedback to change the frequency of the oscillator. This change allows greater system stability and control with changes to the system. The polarization-effect tuning circuit has an open loop feedback design based on the acceleration of the system, as acceleration increases the feedback could increase to the point of instability under open loop design.

The polarization-effect feedback is based entirely on the acceleration of the system, while the IQ modulation technique allows input from the crystal oscillator's phase noise output to correct for the vibration. This innovation allows greater controls over all environmental conditions such as tilt.

Another limitation of the polarization-effect feedback circuit is that the vibration isolation showed little effect at higher frequencies. The IQ modulation phase noise reduction technique was designed to allow phase noise reduction to be improved up to 2.5 kHz. In order to accomplish this, the phase noise integrator was given a wide pass band up beyond 2.5 kHz. In theory, this should improve the overall performance of the system over all phase noise offsets. These design innovations would make this circuit the ideal one for both performance and size to limit the phase noise of the crystal oscillator.

3.10 Future Improvements

Throughout the studies of the design of IQ modulation, phase noise reduction in several other design techniques surfaced that could be used. Since the focus was on the IQ modulation technique these were not studied any further. However, utilizing these circuits could improve further upon the phase noise improvements.

Digital signal processors have improved to speeds of 1.2 GHz, Texas Instrument's C6000 series, over the last several years. Utilizing these circuits could allow faster and more accurate feedback specifically tuned to a specific circuit.

The phase noise integrator and accelerometer can be used as inputs to a digital signal processor chip, which could access a stored memory chip. This memory could include a table of results for the exact voltage based on the level of phase noise integrator and accelerometer to feed back. That voltage could then be sent back into the oscillator directly. This would remove the IQ modulation chain and replace it instead with a digitally tuned memory.

The benefit of this is that it could take into account everything and give a more accurate voltage based on any particular abnormalities seen by the crystal. This would allow more precise feedback control. The downside of this particular design is the effort for the circuitry. The number of circuits on the board would decrease, but the added testing for characterization of the crystal oscillator under different vibration conditions is not always possible.

Another circuit that could be used in this situation is a slope detector. This circuit would have to be tuned to 10 MHz. The theory behind a slope detector is that if the signal is at 10 MHz it will simply go to ground and be 0 Volts. If, however, the circuit strays from the tuned center at all there will be a voltage change at the output based on how much that change is.

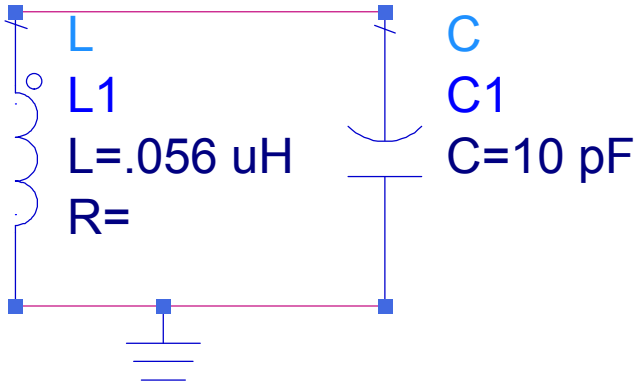

Figure 3-42 10 MHz Slope Detector

In theory, this circuit could be used at the output of the oscillator and as the vibration changed the frequency to create phase noise, this would detect the change and feed back a control voltage based on how far it had to slide to bring the frequency back. Simply adding this circuit to the already implemented IQ modulation scheme is impractical. The Q of the circuit would be very large and the frequency changes measured in the IQ modulation phase noise reduction design are for 0.55 ppm and less, this circuit works best with larger steps away from the center than that.

Conclusion

In the industry of communications the local oscillator has the greatest impact on the overall system phase noise. Vibrating the crystal contained in the oscillator adds phase noise to the system which gets amplified at the transmitted output. To reduce the vibration while maintaining overall size, weight and performance of the communication system as a whole is the goal of this project.

Using a method similar to IQ modulation to combine two channels of data containing different vibration axis data a phase noise coefficient could be extracted and applied to the crystal. This would prevent the frequency of the oscillator from straying as vibration on the system increased. Using the feedback into the crystal to prevent frequency shift allowed a reduction in phase noise and improved overall system performance under vibration.

Vibration levels in military applications are often higher than commercial applications due to the field stress the object receives. For an application in military communications that utilizes crystal oscillators, IQ modulation phase noise reduction is the preferential option. The size and weight of the system would be reduced from that of mechanical isolators. The performance and controllability would be improved from the open loop cancelation designs.

Bibliography

[1] Warren A. Marrison, "The Evolution of the Quartz Crystal Clock," *The Bell System Technical Journal*, Vol. XXVII, pp. 510-588, 1948.

[2] Thomas H. Lee, "It's About Time: A Brief Chronology of Chronometry," *IEEE*, July 2008.

[3] Walter G. Cady, "Method of Maintaining Electric Currents of Constant Frequency," U.S. Patent 1472583, filed 28 May 1921, issued 30 October 1923.

[4] George W. Pierce, "Electrical System," U.S. Patent 1789496, filed 25 February 1924, issued 20 January 1931.

[5] Telestrain Limited, "Phase noise" http://www.telestrian.co.uk/phasenoise.html, 10 December 2009.

[6] Wenzel Associates, Inc, "Vibration-Induced Phase Noise" http://www.wenzel.com/documents/vibration.html, 10 December 2009.

[7] Dimension Engineering LLC, "A beginner's guide to accelerometers" http://www.dimensionengineering.com/accelerometers.htm, 14 December 2009.

[8] http://mechatronics.colostate.edu/figures/9-50.gif, 14 December 2009.

[9] http://lapierre.jammys.net/masters/fig22.gif, 14 December 2009.

[10] Agilent "IQ Modulation", http://education.tm.agilent.com/index.cgi?CONTENT_ID=4, 14 December 2009.

[11] RF Cafe "Quadrature (I/Q) Modulation Modulator Sideband & Carrier Suppression", http://www.rfcafe.com/references/electrical/quad-mod.htm, 14 December 2009.

[12] Aeroflex Isolators, "Aeroflex Isolators for shock and vibration protection in all environments" http://www.vmc-kdc.com/PDFs/wirearx.pdf, 23 December 2009.

[13] Vincent J. Rosati, "Suppression of Vibration-Induced Phase Noise in Crystal Oscillators: An Update" 41st Annual Frequency Control Symposium, 1987.

[14] CTS Electronic Components, INC. "Product Specification 10.000000MHz OCXO" 1960027 Rev A.

[15] Mini-Circuits "Surface Mount Directional Couplers" http://www.minicircuits.com/pdfs/DBTC-12-4+.pdf, 7 January 2010

[16] Joe Wolfe, "RC Filters, integrators and differentiators" http://www.animations.physics.unsw.edu.au/jw/RCfilters.html#integrator, 7 January 2010

[17] Narippawaj Ngernvijit, "Integration Circuit" http://pirun.ku.ac.th/~fscinrn/Nuclear%20Instrument/node107.html, 7 January 2010.

[18] Adel S. Sedra and Kenneth C. Smith, Microelectronic Circuits Fifth Edition Oxford University Press, Oxford New York, 2004 pgs 77-79.

[19] Analog Devices, "Small and Thin ±2g Accelerometer" Norwood, MA 2007

[20] Stephen A Maas, Microwave Mixers Second Edition Artech House, Boston, 1993 pg 319.

Appendix

Table 3 Acronym List

Acronym	Meaning
ADS	Advanced Design System, Rockwell Collins License
C	Capacitor
dB	Decibels
dBc	Decibels Below Carrier Level
DC	Direct Current
g	Gravitational Force
Hz	Hertz
kHz	Kilo Hertz
L	Inductor
mV	Millivolts
PCB	Printed Circuit Board
PM	Phase Modulation
R	Resistor
RF	Radio Frequency
SSB	Single Side Band
V	Volts